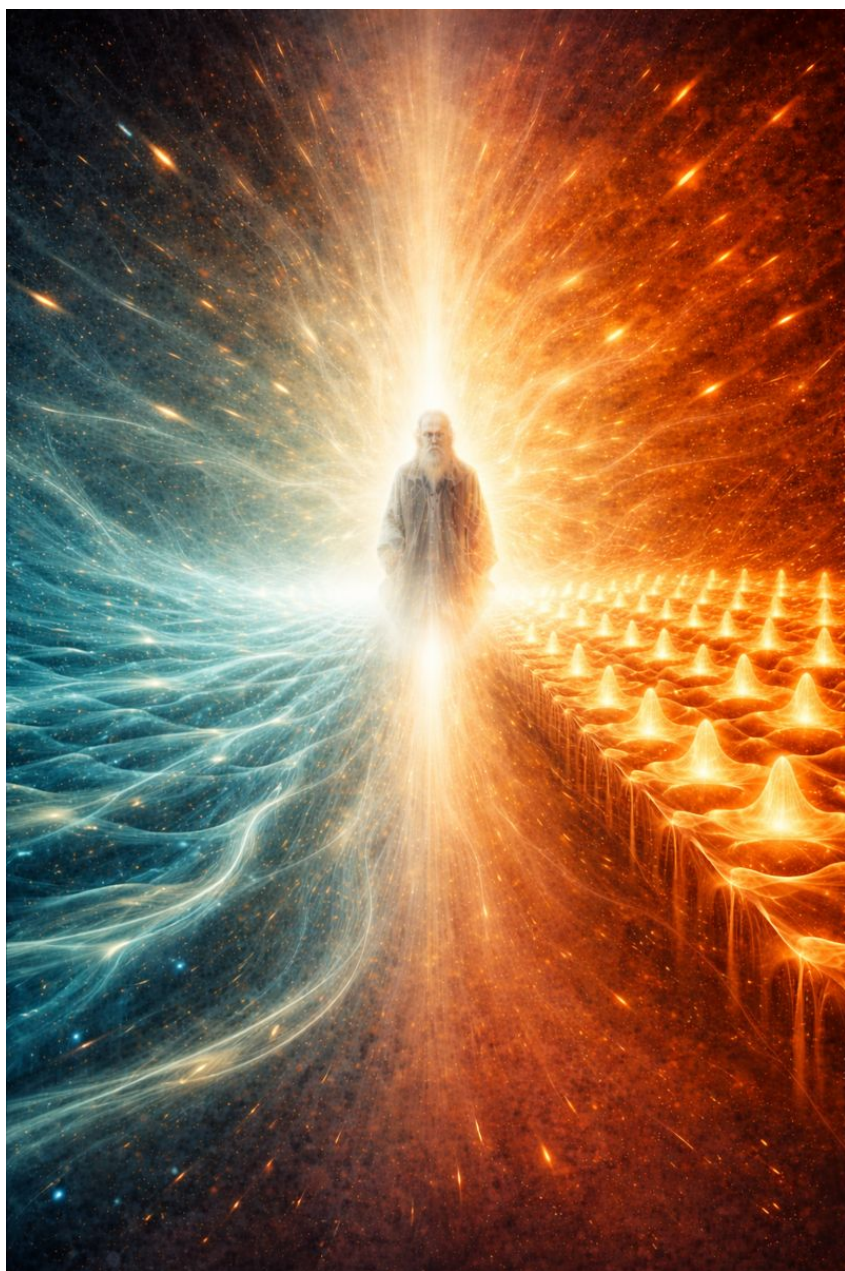


Bose-Hubbard Model

Tristan.W

December 30, 2025



Contents

1	Bose–Hubbard Model: overview and two solvable limits	3
1.1	Model definition and notation	3
1.2	Weak-interaction limit $U \rightarrow 0$: Bose condensation and superfluidity	3
1.3	Strong-interaction limit $J \rightarrow 0$: Mott insulator and charge gap	7
1.4	Why a quantum phase transition is expected	8
2	Quantum phase transitions: scaling, universality, and the critical regime	8
2.1	Definition and comparison with thermal transitions	8
2.2	Second-order QPT: vanishing energy scale and diverging length scale	8
2.3	Long-wavelength effective field theory and universality	9
2.4	Quantum critical regime: breakdown of quasiparticles, and emergent symmetry	9
3	Strong-coupling expansion from the MI side	9
3.1	Particle excitation: degenerate perturbation theory and Bose enhancement	9
3.2	Hole excitation: degenerate perturbation theory	11
3.3	Critical criterion and linear closing of the MI gap	11
3.4	Mott lobe boundary: shape and properties from inequalities	12
4	Mean-field approach from the SF side	13
4.1	Mean-field decoupling and the single-site Hamiltonian	13
4.2	Self-consistency and physical meaning of solutions	14
4.3	Landau expansion near the transition and the mean-field Mott lobes	14
4.4	Mean-field critical scaling	17
5	Effective field theory near criticality and emergent Lorentz symmetry	17
5.1	From coherent-state path integral to the EFT	17
5.2	Ward identity: $U(1)$ symmetry constraint between u and a	18
5.3	Computing u from $a(\mu)$: the particle–hole symmetric line	19
5.4	Emergent Lorentz symmetry: why $u \neq 0$ is nonrelativistic but $u = 0$ is relativistic	19
5.5	Distinct critical behavior: Relativistic vs Nonrelativistic	20
A	Critical scaling of the gap (non-relativistic, away from p–h symmetric point)	21
A.1	Mott-insulator side: strong-coupling gaps and linear closing	21
A.2	Superfluid side: Landau expansion and linear scaling of the low-energy scale . .	22
A.3	Critical Gap Scaling	23
B	Coherent-state path integral: a self-contained derivation	24
B.1	Bosonic coherent states: definitions and identities	24
B.2	From operators to a path integral: Trotter slicing	24
B.3	Derivation of the coherent-state path integral	25
B.4	Many-body generalization and the Bose–Hubbard example	26
C	From coherent-state path integral to a long-wavelength effective action	27

1 Bose–Hubbard Model: overview and two solvable limits

1.1 Model definition and notation

Hamiltonian. The Bose–Hubbard model (Bose–Hubbard model, BHM) is defined on a lattice with bosonic operators $\hat{b}_i, \hat{b}_i^\dagger$ satisfying $[\hat{b}_i, \hat{b}_j^\dagger] = \delta_{ij}$, and on-site number operator $\hat{n}_i \equiv \hat{b}_i^\dagger \hat{b}_i$. The Hamiltonian is

$$\hat{H}_{\text{BH}} = -J \sum_{\langle ij \rangle} (\hat{b}_i^\dagger \hat{b}_j + \text{h.c.}) + \frac{U}{2} \sum_i \hat{n}_i (\hat{n}_i - 1) - \mu \sum_i \hat{n}_i, \quad (1)$$

where J is the nearest-neighbor hopping, $U > 0$ the on-site repulsion, μ the chemical potential, and $\langle ij \rangle$ runs over nearest-neighbor pairs. The coordination number is denoted by Z .

Let N_s be the number of lattice sites and N the total particle number. The average filling is

$$n \equiv \frac{N}{N_s} = \langle \hat{n}_i \rangle \quad (\text{uniform states}). \quad (2)$$

Two phases already visible from limits. The limits $U \rightarrow 0$ (kinetic-energy dominated) and $J \rightarrow 0$ (interaction dominated) lead to qualitatively different ground states: a superfluid (SF) with long-range phase coherence versus a Mott insulator (MI) with a charge gap and fixed integer filling.

1.2 Weak-interaction limit $U \rightarrow 0$: Bose condensation and superfluidity

Set $U = 0$: free bosons on a lattice. With $U = 0$, the Hamiltonian becomes

$$\hat{H}_{U=0} = -J \sum_{\langle ij \rangle} (\hat{b}_i^\dagger \hat{b}_j + \text{h.c.}) - \mu \sum_i \hat{n}_i, \quad (3)$$

which is quadratic and diagonalizable in momentum space (Bloch basis).

Bose-condensation as ground state wavefunction.

At zero temperature, noninteracting bosons minimize energy by putting all particles into the single-particle ground state. On a translationally invariant lattice, the lowest Bloch state is at quasi-momentum $k = 0$.

The $k = 0$ mode is the equal-phase superposition of Wannier orbitals¹:

$$\hat{b}_{k=0}^\dagger = \frac{1}{\sqrt{N_s}} \sum_{i=1}^{N_s} \hat{b}_i^\dagger. \quad (4)$$

A number-conserving condensate with total particle number N is

$$|\text{SF}\rangle = \frac{1}{\sqrt{N!}} \left(\frac{1}{\sqrt{N_s}} \sum_{i=1}^{N_s} \hat{b}_i^\dagger \right)^N |0\rangle. \quad (5)$$

Exactly diagonalizing $\hat{H}_{U=0}$ in momentum space

Assume a translationally invariant lattice with periodic boundary conditions (Born–von

¹Remember the general Fourier Transformation Formula: $\hat{b}_k^\dagger = \frac{1}{\sqrt{N_s}} \sum_{i=1}^{N_s} e^{ik \cdot r_i} \hat{b}_i^\dagger$.

Karman). Define the lattice Fourier transform (here i labels sites at positions \mathbf{r}_i):

$$\hat{b}_i = \frac{1}{\sqrt{N_s}} \sum_k e^{ik \cdot \mathbf{r}_i} \hat{b}_k, \quad \hat{b}_k = \frac{1}{\sqrt{N_s}} \sum_i e^{-ik \cdot \mathbf{r}_i} \hat{b}_i, \quad (6)$$

so that $[\hat{b}_k, \hat{b}_{k'}^\dagger] = \delta_{k,k'}$. The number term is immediately diagonal:

$$\sum_i \hat{n}_i = \sum_i \hat{b}_i^\dagger \hat{b}_i = \sum_k \hat{b}_k^\dagger \hat{b}_k. \quad (7)$$

Hopping term. For the nearest-neighbor hopping, write the neighbor positions as $\mathbf{r}_j = \mathbf{r}_i + \boldsymbol{\delta}$, where $\boldsymbol{\delta}$ runs over the Z nearest-neighbor vectors. Then

$$\sum_{\langle ij \rangle} \hat{b}_i^\dagger \hat{b}_j = \sum_i \sum_{\boldsymbol{\delta} \in \text{n.n.}} \hat{b}_i^\dagger \hat{b}_{i+\boldsymbol{\delta}}. \quad (8)$$

Substitute the Fourier expansion:

$$\sum_i \sum_{\boldsymbol{\delta}} \hat{b}_i^\dagger \hat{b}_{i+\boldsymbol{\delta}} = \sum_i \sum_{\boldsymbol{\delta}} \left(\frac{1}{\sqrt{N_s}} \sum_k e^{-ik \cdot \mathbf{r}_i} \hat{b}_k^\dagger \right) \left(\frac{1}{\sqrt{N_s}} \sum_{k'} e^{ik' \cdot (\mathbf{r}_i + \boldsymbol{\delta})} \hat{b}_{k'} \right) \quad (9)$$

$$= \frac{1}{N_s} \sum_{k, k'} \left(\sum_i e^{i(k' - k) \cdot \mathbf{r}_i} \right) \left(\sum_{\boldsymbol{\delta}} e^{i \boldsymbol{\delta} \cdot \mathbf{r}_i} \right) \hat{b}_k^\dagger \hat{b}_{k'}. \quad (10)$$

Using the discrete orthogonality $\sum_i e^{i(k' - k) \cdot \mathbf{r}_i} = N_s \delta_{k,k'}$, we obtain

$$\sum_{\langle ij \rangle} \hat{b}_i^\dagger \hat{b}_j = \sum_k \left(\sum_{\boldsymbol{\delta}} e^{i \boldsymbol{\delta} \cdot \mathbf{r}_i} \right) \hat{b}_k^\dagger \hat{b}_k. \quad (11)$$

Adding the Hermitian conjugate gives a real dispersion:

$$\sum_{\langle ij \rangle} (\hat{b}_i^\dagger \hat{b}_j + \text{h.c.}) = \sum_k \varepsilon_k \hat{b}_k^\dagger \hat{b}_k, \quad \varepsilon_k \equiv 2 \sum_{\boldsymbol{\delta}} \cos(k \cdot \boldsymbol{\delta}), \quad (12)$$

where the sum over $\boldsymbol{\delta}$ is over a chosen set of nearest-neighbor vectors (e.g. for a hypercubic lattice, one may take $\boldsymbol{\delta} = \pm a \hat{e}_\alpha$ and then $\varepsilon_k = 2 \sum_{\alpha=1}^d \cos(k_\alpha a)$).

Diagonal form. Therefore the $U = 0$ Hamiltonian is diagonal in k :

$$\hat{H}_{U=0} = \sum_k \xi_k \hat{b}_k^\dagger \hat{b}_k, \quad \xi_k \equiv -J \varepsilon_k - \mu. \quad (13)$$

Matching the BEC ansatz. The single-particle ground state corresponds to the momentum k_0 minimizing ξ_k . For standard lattices with $J > 0$, this minimum is at $k_0 = 0$, hence the many-boson ground state at fixed N is

$$|\text{SF}\rangle = \frac{1}{\sqrt{N!}} (\hat{b}_{k=0}^\dagger)^N |0\rangle, \quad \hat{b}_{k=0}^\dagger = \frac{1}{\sqrt{N_s}} \sum_i \hat{b}_i^\dagger, \quad (14)$$

which is exactly the BEC wavefunction (4) used in the main text.

Particle number distribution and fluctuation.

In this state, the on-site occupation number is approximately Poisson distributed,

$$P(n_i) = e^{-\bar{n}} \frac{\bar{n}^{n_i}}{n_i!}, \quad \bar{n} \equiv \langle \hat{n}_i \rangle. \quad (15)$$

It follows immediately that the number fluctuation on each lattice site is

$$\langle (\delta n_i)^2 \rangle = \langle (\hat{n}_i - \bar{n})^2 \rangle = \bar{n}, \quad (16)$$

which indicates that the particle number exhibits strong on-site fluctuations. A detailed derivation can be found in a box below.

Local number statistics: multinomial → binomial → Poisson

Consider the fixed- N condensate in the uniform $k = 0$ mode,

$$|\Psi_N\rangle = \frac{1}{\sqrt{N!}} \left(\hat{b}_0^\dagger \right)^N |0\rangle, \quad \hat{b}_0^\dagger \equiv \frac{1}{\sqrt{N_s}} \sum_{i=1}^{N_s} \hat{b}_i^\dagger. \quad (17)$$

To extract the weight of a Fock configuration $\{n_i\}$ (with $\sum_i n_i = N$), expand the multinomial

$$\left(\sum_{i=1}^{N_s} \hat{b}_i^\dagger \right)^N = \sum_{\{n_i\} : \sum_i n_i = N} \frac{N!}{\prod_i n_i!} \prod_{i=1}^{N_s} \left(\hat{b}_i^\dagger \right)^{n_i}, \quad (18)$$

where the coefficient $\frac{N!}{\prod_i n_i!}$ counts the number of distinct permutations (assignments) of the N identical creation-operator factors among the N_s sites that realize the same occupation numbers $\{n_i\}$.

Using the normalized site Fock basis

$$|\{n_i\}\rangle \equiv \prod_{i=1}^{N_s} \frac{\left(\hat{b}_i^\dagger \right)^{n_i}}{\sqrt{n_i!}} |0\rangle, \quad \langle \{n_i\} | \{n_i\} \rangle = 1, \quad (19)$$

Eq. (18) implies

$$|\Psi_N\rangle = \sum_{\{n_i\} : \sum_i n_i = N} \underbrace{\sqrt{\frac{N!}{\prod_i n_i!}} \left(\frac{1}{\sqrt{N_s}} \right)^N}_{\text{amplitude for } \{n_i\}} |\{n_i\}\rangle. \quad (20)$$

Therefore the probability of observing an occupation pattern $\{n_i\}$ is the multinomial law

$$P(\{n_i\}) = |\langle \{n_i\} | \Psi_N \rangle|^2 = \frac{N!}{\prod_i n_i!} \left(\frac{1}{N_s} \right)^N, \quad \sum_{\{n_i\} : \sum_i n_i = N} P(\{n_i\}) = 1. \quad (21)$$

Physically, it says that in the fixed- N condensate (all bosons occupying the uniform $k = 0$ orbital), each particle is *delocalized* over the whole lattice and “chooses” any site with the same single-particle probability $1/N_s$.

This viewpoint immediately implies the marginal at one site is binomial: if each boson lands on a chosen site i with probability $p = 1/N_s$ (and lands elsewhere with $1 - p$), then n_i is simply “the number of successes in N trials,” hence

$$P(n_i = m) = \binom{N}{m} p^m (1 - p)^{N-m}, \quad p = \frac{1}{N_s}.$$

Marginal at one site.

Fix a site i . As discussed in the last paragraph, summing $P(\{n_i\})$ over all occupations on the other $N_s - 1$ sites yields the binomial distribution

$$P(n_i = m) = \binom{N}{m} \left(\frac{1}{N_s} \right)^m \left(1 - \frac{1}{N_s} \right)^{N-m}, \quad (22)$$

which has mean and variance

$$\langle \hat{n}_i \rangle = N \frac{1}{N_s} = \bar{n}, \quad \text{Var}(n_i) = N \frac{1}{N_s} \left(1 - \frac{1}{N_s} \right) = \bar{n} \left(1 - \frac{1}{N_s} \right). \quad (23)$$

Thermodynamic limit. Taking $N, N_s \rightarrow \infty$ with $\bar{n} \equiv N/N_s$ fixed (so $p \equiv 1/N_s \rightarrow 0$ and $Np = \bar{n}$ fixed), Eq. (22) reduces to Poisson statistics,

$$P(n_i = m) \xrightarrow[N, N_s \rightarrow \infty]{} e^{-\bar{n}} \frac{\bar{n}^m}{m!}, \quad \langle \hat{n}_i \rangle = \bar{n}, \quad \langle (\delta n_i)^2 \rangle = \bar{n}. \quad (24)$$

Thus, in the condensate the on-site particle number exhibits strong fluctuations of order $\sqrt{\bar{n}}$.

Detailed derivation of marginal distribution at one site is binomial.

Fix a site i and set $n_i = m$. Then

$$P(n_i = m) = \sum_{\{n_{j \neq i}\}: \sum_{j \neq i} n_j = N-m} \frac{N!}{m! \prod_{j \neq i} n_j!} \left(\frac{1}{N_s} \right)^N.$$

Use the identity (a direct consequence of the multinomial theorem)

$$(N_s - 1)^{N-m} = \sum_{\{n_{j \neq i}\}: \sum_{j \neq i} n_j = N-m} \frac{(N-m)!}{\prod_{j \neq i} n_j!} \implies \sum_{\{n_{j \neq i}\}} \frac{1}{\prod_{j \neq i} n_j!} = \frac{(N_s - 1)^{N-m}}{(N-m)!}.$$

Hence

$$P(n_i = m) = \frac{N!}{m!(N-m)!} \left(\frac{1}{N_s} \right)^N (N_s - 1)^{N-m} = \binom{N}{m} \left(\frac{1}{N_s} \right)^m \left(1 - \frac{1}{N_s} \right)^{N-m},$$

which is precisely the binomial law with $p = 1/N_s$.

ODLRO and long-range coherence. The off-diagonal correlator can be computed directly in $|SF\rangle$. Using $\hat{b}_{k=0}|SF\rangle = \sqrt{N}|SF_{N-1}\rangle$ and $\hat{b}_i = \hat{b}_{k=0}/\sqrt{N_s} + \dots^2$, one finds for $i \neq j$,

$$\langle SF | \hat{b}_i^\dagger \hat{b}_j | SF \rangle = \frac{N}{N_s} = \bar{n}, \quad (25)$$

and similarly $\langle \hat{b}_i^\dagger \hat{b}_i \rangle = \bar{n}$. Hence

$$\langle \hat{b}_i^\dagger \hat{b}_j \rangle \rightarrow C \neq 0 \quad (|i - j| \rightarrow \infty), \quad (26)$$

which is the defining feature of off-diagonal long-range order (ODLRO).

Excitations and superfluidity . Turning on weak interactions (U small but nonzero), the Goldstone mode associated with broken $U(1)$ symmetry produces a gapless phonon with linear dispersion at small momentum; a linear low-energy spectrum implies a finite Landau critical velocity and thus superfluidity.

²The terms in "...", namely those finite k modes, annihilate $|SF\rangle$ and thus doesn't contribute to $\langle \hat{b}_i^\dagger \hat{b}_j \rangle$.

1.3 Strong-interaction limit $J \rightarrow 0$: Mott insulator and charge gap

With $J = 0$, the Hamiltonian is a sum of on-site terms:

$$\hat{H}_{J=0} = \sum_i \hat{H}_i, \quad \hat{H}_i = \frac{U}{2} \hat{n}_i (\hat{n}_i - 1) - \mu \hat{n}_i. \quad (27)$$

Each site is independent and \hat{n}_i is a good quantum number.

Ground-state filling n_0 . Let $E(n) = \frac{U}{2}n(n-1) - \mu n$ be the on-site energy at integer n . The optimal filling n_0 satisfies

$$E(n_0) \leq E(n_0 \pm 1). \quad (28)$$

Evaluating the inequalities yields

$$U(n_0 - 1) < \mu < Un_0, \quad (29)$$

so equivalently

$$n_0 = \lfloor \mu/U \rfloor + 1. \quad (30)$$

MI ground state: product of Fock states. The many-body ground state is a product state with fixed integer occupation:

$$|\text{MI}\rangle = \prod_i \frac{1}{\sqrt{n_0!}} (\hat{b}_i^\dagger)^{n_0} |0\rangle. \quad (31)$$

- Each site is an exact number eigenstate: $\langle (\delta n_i)^2 \rangle = 0$, so there is no number fluctuation.
- Since $|\text{MI}\rangle$ has fixed number on each site,

$$\langle \text{MI} | \hat{b}_i^\dagger \hat{b}_j | \text{MI} \rangle = 0 \quad (i \neq j), \quad (32)$$

hence no ODLRO.

Charge excitations: particle and hole.

Two elementary charge excitations are:

- Particle excitation: add one particle at a site, $n_0 \rightarrow n_0 + 1$:

$$\Delta_p^{(0)} = E(n_0 + 1) - E(n_0) = Un_0 - \mu. \quad (33)$$

- Hole excitation: remove one particle at a site, $n_0 \rightarrow n_0 - 1$:

$$\Delta_h^{(0)} = E(n_0 - 1) - E(n_0) = \mu - U(n_0 - 1). \quad (34)$$

Charge gap in the MI. For $U(n_0 - 1) < \mu < Un_0$, both $\Delta_p^{(0)}$ and $\Delta_h^{(0)}$ are positive, so the MI has a finite charge gap

$$\Delta_-^{(0)} = \min\{\Delta_p^{(0)}, \Delta_h^{(0)}\} > 0. \quad (35)$$

At the discrete points $\mu = Un$ (integer n), one of the two gaps closes already at $J = 0$.

Particle-hole symmetric point. Within a given MI lobe, there is a special μ where $\Delta_p^{(0)} = \Delta_h^{(0)}$; this “particle–hole symmetric point” will control a distinct critical behavior when the SF–MI transition is approached along that line.

1.4 Why a quantum phase transition is expected

At least two distinct $T = 0$ phases. The $U \rightarrow 0$ limit has $\langle \hat{b}_i \rangle \neq 0$ (SF), while the $J \rightarrow 0$ limit has $\langle \hat{b}_i \rangle = 0$ and a charge gap (MI). Since these phases differ by an order parameter and by the presence/absence of a gap, they cannot be smoothly connected without a singular change in the ground state in the thermodynamic limit.

Control parameter. We take the dimensionless ratio

$$g \equiv \frac{J}{U} \quad (36)$$

as the tuning parameter. Physically, increasing g enhances kinetic delocalization and on-site number fluctuations, favoring SF order; decreasing g suppresses hopping, favors integer filling, and stabilizes the gapped MI.

2 Quantum phase transitions: scaling, universality, and the critical regime

2.1 Definition and comparison with thermal transitions

Definition (ground-state non-analyticity). A quantum phase transition (QPT) is a zero-temperature transition driven by a Hamiltonian parameter g , at which the ground-state energy density $e_0(g)$ becomes non-analytic (some derivative with respect to g is discontinuous or divergent) in the thermodynamic limit.

Thermal vs quantum. Thermal transitions are driven by temperature and are detected via non-analyticities of the free energy. Quantum transitions are driven by a parameter in \hat{H} and are detected via the ground-state energy; temperature plays the role of a finite-size cutoff in the imaginary-time direction.

2.2 Second-order QPT: vanishing energy scale and diverging length scale

Scaling hypotheses. For a continuous (second-order) QPT, a characteristic low-energy scale Δ vanishes and a correlation length ξ diverges as $g \rightarrow g_c$.

Standard scaling relations.

$$\Delta \sim |g - g_c|^{z\nu}, \quad \xi \sim |g - g_c|^{-\nu}, \quad \Delta \sim \xi^{-z}. \quad (37)$$

Here ν is the correlation-length exponent and z the dynamical critical exponent.

How Δ and ξ appear in the BHM

On the MI side, the natural low-energy scale is the charge gap:

$$\Delta_- \equiv \min\{\Delta_p, \Delta_h\}, \quad (38)$$

which controls the exponential decay of equal-time correlations, $\langle \hat{b}_i^\dagger \hat{b}_j \rangle \sim e^{-|i-j|/\xi_-}$.

On the SF side, there is a gapless Goldstone mode in the low energy regime. Nevertheless one may define a crossover scale Δ_+ separating the linear phonon regime from higher-energy single-particle-like behavior. The associated length scale ξ_+ plays the role of a healing length. At a continuous SF-MI transition, both Δ_- and Δ_+ vanish as $g \rightarrow g_c$, and both ξ_- and ξ_+ diverge.

2.3 Long-wavelength effective field theory and universality

Why an effective continuum theory exists. Near criticality, $\xi \gg a$ (lattice spacing), so the long-distance physics is controlled by a coarse-grained order-parameter field theory. The same effective theory governs both sides of the transition in the scaling limit.

Universality. Microscopic details (lattice geometry, further-neighbor hopping, etc.) shift the location g_c and non-universal prefactors, but do not change critical exponents such as z and ν , which are fixed by the universality class of the long-wavelength theory.

2.4 Quantum critical regime: breakdown of quasiparticles, and emergent symmetry

Finite temperature above the QCP. Strictly, QPTs are defined at $T = 0$, but experimentally and theoretically one often probes a finite-temperature “quantum critical” regime above g_c , controlled by the same low-energy fixed point.

Why quasiparticles may fail. When the only intrinsic scales Δ and ξ^{-1} vanish, low-energy excitations can become strongly damped; a sharp quasiparticle description need not exist. Instead, one expects scaling forms for correlators controlled by the fixed point.

Emergent symmetry. The low-energy fixed point may have a larger symmetry than the microscopic Hamiltonian (“emergent symmetry”). A central example in the BHM is the emergent Lorentz symmetry along the particle–hole symmetric line, discussed in Section 5.

3 Strong-coupling expansion from the MI side

Strategy :MI as the reference point.

In the MI, charge excitations are fully gapped; the SF–MI transition can be located by the closing of the charge gap. The strong-coupling expansion starts from $J \rightarrow 0$, where particle/hole excitations on different sites are degenerate³. finite J couples these degenerate states, lowers the excitation energy, and eventually closes the gap.

3.1 Particle excitation: degenerate perturbation theory and Bose enhancement

Degenerate subspace at $J = 0$. Define single-particle excitation states

$$|p\rangle_i \propto \hat{b}_i^\dagger |\text{MI}\rangle, \quad (39)$$

or write it in a normalized form⁴,

$$|p\rangle_i \equiv \frac{1}{\sqrt{n_0 + 1}} \hat{b}_i^\dagger |\text{MI}\rangle = |n_0 + 1\rangle_i \prod_{j \neq i} |n_0\rangle_j. \quad (40)$$

The unperturbed excitation energy is

$$\Delta_p^{(0)} = Un_0 - \mu. \quad (41)$$

All $|p\rangle_i$ are degenerate for different i .

When a perturbation J –term is added to the Hamiltonian, one can easily calculate the matrix element with the single-particle excitation state. See the box below.

³Particle excitation and hole excitation are not degenerate. Particle excitations at different sites are degenerate, and the same applies for hole excitations.

⁴Remember n_0 is defined in Eq. (30) as the ground state occupation number.

Computing the hopping matrix element $\langle p_j | \hat{H}_t | p_i \rangle$

Let $\hat{H}_t = -J \sum_{\langle \ell m \rangle} (\hat{b}_\ell^\dagger \hat{b}_m + \text{h.c.})$. For nearest neighbors $\langle ij \rangle$,

$$\langle p_j | \hat{H}_t | p_i \rangle = -J \langle \text{MI} | \hat{b}_j (\hat{b}_j^\dagger \hat{b}_i) \hat{b}_i^\dagger | \text{MI} \rangle. \quad (42)$$

Using on-site actions $\hat{b}|n\rangle = \sqrt{n}|n-1\rangle$, $\hat{b}^\dagger|n\rangle = \sqrt{n+1}|n+1\rangle$, the relevant local factors are: at site i : $\hat{b}_i \hat{b}_i^\dagger |n_0\rangle = (n_0+1)|n_0\rangle$; at site j : $\hat{b}_j \hat{b}_j^\dagger |n_0\rangle = (n_0+1)|n_0\rangle$. Note that Eq. (42) is non-zero only when i and j are adjacent. Hence

$$\langle p_j | \hat{H}_t | p_i \rangle = -J(n_0+1) \quad (\langle ij \rangle), \quad (43)$$

and it vanishes if i, j are not nearest neighbors. The factor n_0+1 is the Bose enhancement factor in the MI background.

Equivalent tight-binding model and leading correction to the particle gap.

Since the hopping matrix element reads $\langle p_i | \hat{H}_J | p_j \rangle = -J(n_0+1)$ for nearest neighbors $\langle ij \rangle$ and 0 otherwise.

Eq. (43) is exactly the tight-binding Hamiltonian

$$\hat{H}_p = \Delta_p^{(0)} \sum_i |p\rangle_i \langle p| - J(n_0+1) \sum_{\langle ij \rangle} (|p\rangle_i \langle p| + |p\rangle_j \langle p|). \quad (44)$$

With periodic boundary conditions the Bloch states $|p, k\rangle = \frac{1}{\sqrt{N_s}} \sum_i e^{ik \cdot r_i} |p\rangle_i$ diagonalize \hat{H}_p , with dispersion

$$E_p(k) = \Delta_p^{(0)} - J(n_0+1) \gamma(k), \quad \gamma(k) \equiv \sum_{\delta \in \text{n.n.}} e^{ik \cdot \delta}. \quad (45)$$

Since $\gamma(\mathbf{0}) = Z$ (coordination number) and $\gamma(k) \leq Z$, the minimum occurs at $k = \mathbf{0}$, so the leading corrected particle gap is

$$\Delta_p = \min_k E_p(k) = \Delta_p^{(0)} - ZJ(n_0+1) = Un_0 - \mu - ZJ(n_0+1), \quad (46)$$

while the ground state is the uniform superposition of all single particle states

$$|p, k=0\rangle = \frac{1}{\sqrt{N_s}} \sum_i |p\rangle_i$$

Why the ground state is the uniform superposition and why the energy shift is $-ZJ(n_0+1)$

In the site basis $\{|p\rangle_i\}$, the hopping part of \hat{H}_p is $-tA$ with $t \equiv J(n_0+1) > 0$ and A the adjacency matrix. For any crystal momentum k Bloch state,

$$\gamma(k) = \sum_{\delta \in \text{n.n.}} e^{ik \cdot \delta} \quad \Rightarrow \quad \gamma(k) \leq \sum_{\delta \in \text{n.n.}} |e^{ik \cdot \delta}| = Z,$$

with equality only at $k = \mathbf{0}$ where all phases align. Therefore $E_p(k) = \Delta_p^{(0)} - t\gamma(k)$ is minimized at $k = \mathbf{0}$, i.e. the uniform superposition $|p, \mathbf{0}\rangle \propto \sum_i |p\rangle_i$ is the ground state. At $k = \mathbf{0}$, $\gamma(\mathbf{0}) = Z$, giving the maximal kinetic-energy lowering $-tZ = -ZJ(n_0+1)$.

3.2 Hole excitation: degenerate perturbation theory

Degenerate subspace at $J = 0$. Define single-hole excitation states

$$|h\rangle_i \equiv \hat{b}_i |\text{MI}\rangle, \quad (47)$$

with unperturbed energy

$$\Delta_h^{(0)} = \mu - U(n_0 - 1). \quad (48)$$

Computing $\langle h_j | \hat{H}_t | h_i \rangle$

For nearest neighbors $\langle ij \rangle$,

$$\langle h_j | \hat{H}_t | h_i \rangle = -J \langle \text{MI} | \hat{b}_j^\dagger (\hat{b}_j^\dagger \hat{b}_i) \hat{b}_i | \text{MI} \rangle. \quad (49)$$

The hole motion corresponds to moving a background boson into the empty slot. The local factors now involve $\sqrt{n_0}$ rather than $\sqrt{n_0 + 1}$: removing a boson from an n_0 site gives $\sqrt{n_0}$, and adding it back gives $\sqrt{n_0}$. Hence

$$\langle h_j | \hat{H}_t | h_i \rangle = -J n_0 \quad (\langle ij \rangle). \quad (50)$$

Corrected hole gap. The lowest-energy hole state again sits at $k = 0$, yielding

$$\Delta_h = \Delta_h^{(0)} - Z J n_0 = \mu - U(n_0 - 1) - Z J n_0. \quad (51)$$

■ **Comment: Higher-order corrections.** Systematic improvements include multi-particle/hole intermediate states (higher-order in J/U). For locating the phase boundary and understanding the lobe structure, the leading degenerate splitting already captures the key geometry.

3.3 Critical criterion and linear closing of the MI gap

Charge-gap closing criterion.

For fixed μ/U , the MI becomes unstable when the charge gap closes:

$$\Delta_- \equiv \min\{\Delta_p, \Delta_h\} = 0. \quad (52)$$

Thus the phase boundary is determined by either $\Delta_p = 0$ (particle-driven) or $\Delta_h = 0$ (hole-driven).

Linear closing near the boundary.

At this leading order, Δ_p and Δ_h are linear in J , so expanding near $J = J_c$ gives the *linear* expansion relationship:

$$\Delta_- \propto |J - J_c| \iff \Delta_- \propto \left| \frac{J}{U} - \left(\frac{J}{U} \right)_c \right|. \quad (53)$$

We make a short comment on this linear expansion. This relation can be easily seen from Eq. (46) and (51), since they are both linear in J (and thus linear in J/U)⁵. For a more detailed discussion (and derivation) of the critical scaling, refer to Appendix A.

⁵The reason we consider J/U is that J/U is the conventional driving parameter of the MI-SF phase transition

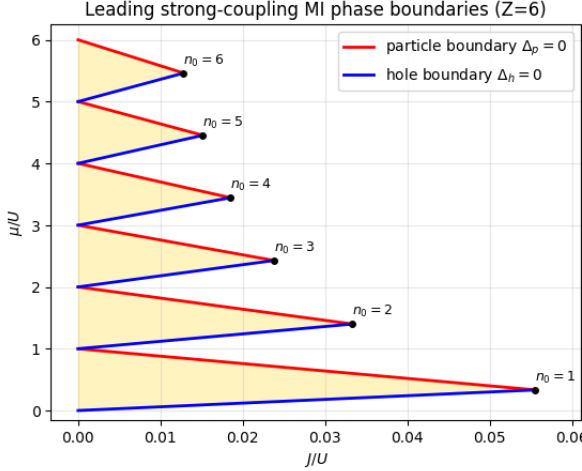


Figure 1: Mott Lobe from Strong-coupling expansion

3.4 Mott lobe boundary: shape and properties from inequalities

Explicit boundary curves (leading strong-coupling). Setting $\Delta_p = 0$ and $\Delta_h = 0$ gives two lines:

$$\Delta_p = 0 : \mu = Un_0 - ZJ(n_0 + 1), \quad (54)$$

$$\Delta_h = 0 : \mu = U(n_0 - 1) + ZJn_0. \quad (55)$$

The MI region at filling n_0 is the set of (μ, J) satisfying $\Delta_p > 0$ and $\Delta_h > 0$, i.e.

$$U(n_0 - 1) + ZJn_0 < \mu < Un_0 - ZJ(n_0 + 1). \quad (56)$$

This finite-gap condition delineates the *Mott-insulating* domain and its phase boundaries. A more explicit derivation is provided in the box below. Throughout, we present the phase diagram in the (x, y) plane with $x \equiv J/U$ and $y \equiv \mu/U$; see Fig. 1. The figure displays a sequence of triangular regions⁶, known as the *Mott lobes*. In the $J = 0$ limit, one recovers Eq. (30),

$$n_0 = \lfloor \mu/U \rfloor + 1, \quad (57)$$

namely the filling is pinned to an integer over each interval of μ/U . As J increases, the upper boundary (where the particle excitation becomes gapless) and the lower boundary (where the hole excitation becomes gapless) move toward each other and the lobe shrinks, until they meet at the lobe tip

$$\frac{J_\star}{U} = \frac{1}{Z(2n_0 + 1)}, \quad \frac{\mu_\star}{U} = \frac{2n_0^2 - 1}{2n_0 + 1}. \quad (58)$$

Note that J_\star decreases with increasing n_0 , so the lobes become progressively smaller as one moves upward to higher fillings.

Detailed Derivation of Mott Lobe Boundary (Strong-Coupling Approach)

Starting from the strong-coupling (atomic-limit) particle and hole gaps, the MI condition $\Delta_p > 0$ and $\Delta_h > 0$ yields

$$U(n_0 - 1) + ZJn_0 < \mu < Un_0 - ZJ(n_0 + 1). \quad (59)$$

⁶The triangular shape is only the leading-order result of the strong-coupling expansion; beyond leading order the lobe boundaries become smooth/rounded.

The *upper* boundary corresponds to a gapless particle excitation, $\Delta_p = 0$, hence it is a μ vs J line with *negative* slope:

$$\mu_p(J) = Un_0 - ZJ(n_0 + 1). \quad (60)$$

The *lower* boundary corresponds to a gapless hole excitation, $\Delta_h = 0$, hence it is a μ vs J line with *positive* slope:

$$\mu_h(J) = U(n_0 - 1) + ZJn_0. \quad (61)$$

The lobe tip is the intersection $\mu_p(J_\star) = \mu_h(J_\star)$, giving

$$\frac{J_\star}{U} = \frac{1}{Z(2n_0 + 1)}, \quad \frac{\mu_\star}{U} = n_0 - \frac{n_0 + 1}{2n_0 + 1} = \frac{2n_0^2 - 1}{2n_0 + 1}. \quad (62)$$

Finally, in the $J \rightarrow 0$ limit the inequalities reduce to $U(n_0 - 1) < \mu < Un_0$, which implies $\mu/U \in (n_0 - 1, n_0)$ and therefore $n_0 = \lfloor \mu/U \rfloor + 1$, consistent with Eq. (30).

Three robust features of the lobe.

- At $\mu = Un_0$, one of the gaps is already zero at $J = 0$, so an infinitesimal J immediately destroys the MI.
- The lobe is most stable near the middle where particle and hole gaps are both large; the upper part is particle-driven ($\Delta_p \rightarrow 0$), the lower part hole-driven ($\Delta_h \rightarrow 0$).
- Bose enhancement (n_0 and $n_0 + 1$) amplifies the effect of hopping at larger n_0 , suppressing J_c/U ; higher-filling lobes are smaller.

4 Mean-field approach from the SF side

Why mean-field can work.

The SF is characterized by a nonzero coherent amplitude on each site. If phase coherence is long-ranged, one may approximate the influence of neighboring sites on a given site by a classical field proportional to $\langle \hat{b} \rangle$. This motivates a mean-field decoupling of the hopping term, reducing the lattice problem to a single-site self-consistent problem (exact in infinite coordination and often qualitatively reliable in higher dimensions).

4.1 Mean-field decoupling and the single-site Hamiltonian

Decoupling the hopping. Use

$$\hat{b}_i^\dagger \hat{b}_j \approx \hat{b}_i^\dagger \langle \hat{b}_j \rangle + \langle \hat{b}_i^\dagger \rangle \hat{b}_j - \langle \hat{b}_i^\dagger \rangle \langle \hat{b}_j \rangle. \quad (63)$$

Assuming a uniform solution $\langle \hat{b}_i \rangle = \psi$ ⁷, define a convenient parameter

$$\phi \equiv ZJ\psi. \quad (64)$$

Then the mean-field Hamiltonian becomes a sum of identical on-site terms,

$$\hat{H}_{\text{MF}} = -\phi \hat{b}^\dagger - \phi^* \hat{b} + \frac{U}{2} \hat{n}(\hat{n} - 1) - \mu \hat{n} + \frac{|\phi|^2}{ZJ}. \quad (65)$$

⁷Obviously ψ can take complex values, i.e. $\psi \in \mathbb{C}$

4.2 Self-consistency and physical meaning of solutions

Self-consistency equation. Let $|\Psi_0(\phi)\rangle$ be the ground state of $\hat{H}_{\text{MF}}(\phi)$. The self-consistency condition reads

$$\psi = \langle \Psi_0(\phi) | \hat{b} | \Psi_0(\phi) \rangle, \quad \phi = ZJ\psi, \quad (66)$$

so equivalently ϕ must satisfy a closed fixed-point equation.

- **MI solution:** If $\phi = 0$, then \hat{H}_{MF} reduces to the $J = 0$ on-site problem; the ground state is a Fock state $|n_0\rangle$ with no number fluctuation and no ODLRO \Rightarrow MI order.

- **SF solution:** If a stable solution with $\phi \neq 0$ exists, \hat{H}_{MF} mixes different $|n\rangle$ on each site, allowing number fluctuations and yielding $\psi = \langle \hat{b} \rangle \neq 0 \Rightarrow$ SF order.

Condensate fraction and ϕ

The physically transparent order parameter is $\psi = \langle \hat{b} \rangle$. In mean-field, inter-site correlations factorize: $\langle \hat{b}_i^\dagger \hat{b}_j \rangle \approx \langle \hat{b}_i^\dagger \rangle \langle \hat{b}_j \rangle = |\psi|^2$ for $i \neq j$. Then the condensate fraction is

$$\frac{N_0}{N} = \frac{1}{NN_s} \sum_{ij} \langle \hat{b}_i^\dagger \hat{b}_j \rangle \approx \frac{N_s}{N} |\psi|^2 = \frac{|\psi|^2}{n}. \quad (67)$$

If one uses $\phi = ZJ\psi$ as the mean-field parameter, then

$$\frac{N_0}{N} \approx \frac{|\phi|^2}{nZ^2J^2}. \quad (68)$$

Thus $\phi \neq 0$ is equivalent to a nonzero condensate fraction, but ϕ itself has energy units.

BCS vs BHM mean-field .

BCS mean-field	BHM mean-field
Pair scattering between $(k \uparrow, -k \downarrow)$ and $(k' \uparrow, -k' \downarrow)$.	Boson hopping between neighboring sites.
Order parameter couples as $\Delta c_{k\uparrow}^\dagger c_{-k\downarrow}^\dagger + \text{h.c.}$	Order parameter couples as $-\phi \hat{b}^\dagger - \phi^* \hat{b}$.
Diagonal in momentum space; quadratic at each k .	Diagonal in real space; interacting on each site but easily solvable numerically.
Self-consistency gives the gap equation.	Self-consistency gives $\phi = ZJ\langle \hat{b} \rangle$.

4.3 Landau expansion near the transition and the mean-field Mott lobes

Landau form. Assuming a continuous transition, expand the ground-state energy density (per site) in small ϕ :

$$\mathcal{E}(\phi) = \mathcal{E}_0 - a|\phi|^2 + b|\phi|^4 + \dots \quad (69)$$

The sign of a determines whether ϕ condenses.

Detailed Derivation: Second-order perturbation theory for $a(\mu, J)$

Split $\hat{H}_{\text{MF}} = \hat{H}_0 + \hat{V}$ with

$$\hat{H}_0 = \frac{U}{2} \hat{n}(\hat{n} - 1) - \mu \hat{n}, \quad \hat{V} = -\phi \hat{b}^\dagger - \phi^* \hat{b} + \frac{|\phi|^2}{ZJ}. \quad (70)$$

Note that the unperturbed Hamiltonian is exactly Eq. (27), i.e. the $J \rightarrow 0$ limit Hamiltonian (in the MI phase). Choose the corresponding MI number state $|n_0\rangle$ as the unperturbed ground state, valid when ϕ is small. The constant term contributes $+|\phi|^2/(ZJ)$ to the energy.

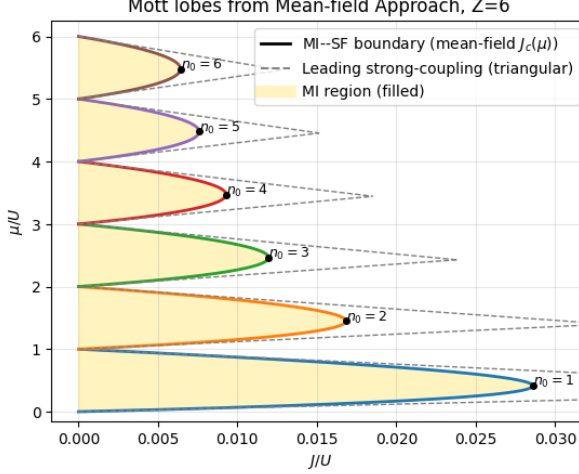


Figure 2: Mott Lobe from Mean-Field Approach. We also present the Strong-Coupling expansion result in gray dashed line.

The linear term has $\langle n_0 | \hat{b} | n_0 \rangle = 0$, so the first nontrivial correction is second order:

$$E^{(2)} = \sum_{m \neq n_0} \frac{|\langle m | (-\phi \hat{b}^\dagger - \phi^* \hat{b}) | n_0 \rangle|^2}{E(n_0) - E(m)}. \quad (71)$$

Only $m = n_0 + 1$ and $m = n_0 - 1$ contribute:

$$\langle n_0 + 1 | \hat{b}^\dagger | n_0 \rangle = \sqrt{n_0 + 1}, \quad \langle n_0 - 1 | \hat{b} | n_0 \rangle = \sqrt{n_0}. \quad (72)$$

Using $E(n_0 + 1) - E(n_0) = Un_0 - \mu$ and $E(n_0) - E(n_0 - 1) = \mu - U(n_0 - 1)$, one finds

$$E^{(2)} = -|\phi|^2 \left(\frac{n_0 + 1}{Un_0 - \mu} + \frac{n_0}{\mu - U(n_0 - 1)} \right). \quad (73)$$

Therefore, the coefficient of $-|\phi|^2$ in \mathcal{E} is^a

$$a = \frac{n_0 + 1}{Un_0 - \mu} + \frac{n_0}{\mu - U(n_0 - 1)} - \frac{1}{ZJ}. \quad (74)$$

^aDon't forget the $|\phi|^2/(ZJ)$ constant energy shift.

Critical condition and lobe boundary.

In Landau theory, $a > 0$ favors $\phi \neq 0$ (SF) and $a < 0$ favors $\phi = 0$ (MI). Thus the phase boundary is $a = 0$, giving

$$\frac{J_c}{U} = \frac{(n_0 - \mu/U)(\mu/U - (n_0 - 1))}{Z(\mu/U + 1)}. \quad (75)$$

This reproduces the familiar Mott lobes at mean-field level; see Fig. 2. Note that the lobe shape here differs from the leading strong-coupling result in Eq. (56). Indeed, Eq. (75) implies that for fixed n_0 , J_c is a parabola-like function of μ , yielding a smooth and rounded lobe boundary rather than a sharp triangle.

Nevertheless, Eqs. (56) and (75) lead to consistent qualitative physics: **(i)** in the $J \rightarrow 0$ limit they agree on the allowed μ -window for the n_0 -th Mott plateau, reproducing Eq. (30); **(ii)** the lobe size shrinks as n_0 increases.

Detailed Derivation of Mott Lobe Boundary (Mean-Field Approach)

Let $y \equiv \mu/U$ and $x \equiv J/U$. The mean-field phase boundary is

$$x_c(y) = \frac{(n_0 - y)(y - (n_0 - 1))}{Z(y + 1)}. \quad (76)$$

(1) The lobe tip.

The lobe *tip* corresponds to the maximal $x_c(y)$ for $y \in (n_0 - 1, n_0)$. Setting $\frac{dx_c}{dy} = 0$ gives

$$y_\star = -1 + \sqrt{n_0(n_0 + 1)} \implies \frac{\mu_\star}{U} = -1 + \sqrt{n_0(n_0 + 1)}. \quad (77)$$

Substituting y_\star back yields the maximal hopping

$$\frac{J_\star}{U} = \frac{2n_0 + 1 - 2\sqrt{n_0(n_0 + 1)}}{Z} = \frac{(\sqrt{n_0 + 1} - \sqrt{n_0})^2}{Z}. \quad (78)$$

It's natural to notice the following inequality:

$$(\sqrt{n_0 + 1} - \sqrt{n_0})^2 = \frac{1}{(\sqrt{n_0 + 1} + \sqrt{n_0})^2} = \frac{1}{2n_0 + 1 + 2\sqrt{n_0(n_0 + 1)}} < \frac{1}{2n_0 + 1},$$

where the last expression correspond to J_\star/U in the Strong-coupling expansion, as shown in Eq. (58).

Thus, J_\star is *smaller* than the leading strong-coupling triangular estimate

$$\left(\frac{J_\star}{U}\right)_{\text{MF}} < \left(\frac{J_\star}{U}\right)_{\text{SC, leading}}. \quad (79)$$

See Fig 2 for comparison. Thus, mean-field predicts a more restrictive MI stability region (a smaller lobe tip).

(2) Endpoints: $J \rightarrow 0$ limit.

At $x = 0$ the MI condition is simply $n_0 - 1 < y < n_0$, namely

$$U(n_0 - 1) < \mu < Un_0. \quad (80)$$

Therefore the filling is pinned to $n_0 = \lfloor \mu/U \rfloor + 1$, consistent with Eq. (30).

(3) Matching the strong-coupling slopes near $J = 0$.

To compare with the linear strong-coupling boundaries, expand $x_c(y)$ near the endpoints. Near the *upper* endpoint, set $y = n_0 - \delta$ with $\delta \ll 1$. Then

$$x_c(y) = \frac{\delta(1 - \delta)}{Z(n_0 + 1 - \delta)} = \frac{\delta}{Z(n_0 + 1)} + O(\delta^2), \quad (81)$$

so $\delta \approx Z(n_0 + 1)x$, i.e.

$$y \approx n_0 - Z(n_0 + 1)x, \quad (82)$$

which matches the strong-coupling particle boundary $\Delta_p = 0$.

Near the *lower* endpoint, set $y = (n_0 - 1) + \delta$ with $\delta \ll 1$. Then

$$x_c(y) = \frac{(1 - \delta)\delta}{Z(n_0 + \delta)} = \frac{\delta}{Zn_0} + O(\delta^2), \quad (83)$$

so $\delta \approx Zn_0 x$, i.e.

$$y \approx (n_0 - 1) + Zn_0 x, \quad (84)$$

which matches the strong-coupling hole boundary $\Delta_h = 0$. Hence the mean-field boundary is tangent to the leading strong-coupling straight lines in the vicinity of $J = 0$, while rounding off the cusp into a smooth tip at larger J .

■ Limits of the two approaches (Strong-coupling expansion and mean field).

The discrepancy between Eq. (56) (triangular lobes) and Eq. (75) (rounded lobes) is expected, since the two approaches implement different controlled approximations. The “strong-coupling” result is the leading $O(J/U)$ expansion of the particle/hole gaps deep in the Mott phase, keeping only the lowest-order hopping processes; higher-order virtual processes $O(J^2/U)$ and beyond, which become increasingly important near the lobe tip where the gap collapses, are neglected and would smooth the cusp into a rounded tip. In contrast, the mean-field/Landau treatment is formulated as a stability analysis of the $\phi = 0$ Mott state against the onset of superfluid order, so it naturally yields a smooth critical line, but it also suppresses spatial/quantum fluctuations and therefore typically *underestimates* the Mott stability (e.g. a smaller J_*). Consequently, the strong-coupling boundary is most reliable for $J/U \ll 1$ (large gap, away from the tip), while mean-field captures the qualitative structure of the phase boundary but is quantitatively accurate only when fluctuations are weak (e.g. in sufficiently high dimensions).

4.4 Mean-field critical scaling

Near the transition on the SF side, minimizing $\mathcal{E}(\phi)$ gives

$$|\phi|^2 \propto a \propto \left| \frac{J}{U} - \left(\frac{J}{U} \right)_c \right|. \quad (85)$$

Accordingly, the condensate fraction N_0/N scales linearly with a (up to the conversion between ϕ and ψ).

Within mean-field, the superfluid low-energy scale Δ_+ tracks the stiffness/condensate amplitude⁸, hence vanishes linearly

$$\Delta_+ \propto \left| \frac{J}{U} - \left(\frac{J}{U} \right)_c \right|. \quad (86)$$

Combined with the strong-coupling result (53) that Δ_- closes linearly, one has a consistent picture away from the particle–hole symmetric line.

5 Effective field theory near criticality and emergent Lorentz symmetry

5.1 From coherent-state path integral to the EFT

A detailed discussion of *coherent-state path integral* is included in Appendix B, and a following derivation of the *effective field theory* is shown in Appendix C.

Two core conclusions from the appendices.

First, we studied the partition function of the Bose–Hubbard model and derived its coherent-state path-integral representation:

$$\mathcal{Z}_{\text{BHM}} = \int_{\text{PBC}} \mathcal{D}[b^*, b] e^{-S_{\text{BHM}}[b^*, b]}, \quad b_i(\beta) = b_i(0), \quad (87)$$

with the Euclidean action

$$S_{\text{BHM}}[b^*, b] = \int_0^\beta d\tau \left[\sum_i b_i^*(\tau) \partial_\tau b_i(\tau) - J \sum_{\langle ij \rangle} (b_i^*(\tau) b_j(\tau) + \text{c.c.}) + \sum_i \left(\frac{U}{2} |b_i(\tau)|^4 - \mu |b_i(\tau)|^2 \right) \right]. \quad (88)$$

⁸In Landau paradigm, if the coefficient of $|\phi|^2$ is a , then $\Delta \propto a$. A more detailed derivation can be found in Appendix A.

These are precisely Eqs. (158) and (162). More generally, we may write the lattice action in the split form

$$S[b^*, b] = S_{\text{loc}}[b^*, b] - \int_0^\beta d\tau \sum_{ij} b_i^*(\tau) t_{ij} b_j(\tau), \quad (89)$$

as in Eq. (160), where $S_{\text{loc}} = \sum_i S_{0,i}$ contains only on-site terms (cf. Eq. (161)).

From the lattice coherent-state path integral (87), a Hubbard–Stratonovich decoupling of the hopping term rewrites the partition function exactly as

$$\mathcal{Z} \propto \int \mathcal{D}[\phi^*, \phi] e^{-S_{\text{eff}}[\phi^*, \phi]}, \quad S_{\text{eff}}[\phi^*, \phi] = \int_0^\beta d\tau \phi^\dagger t^{-1} \phi - \sum_i \ln \mathcal{Z}_{\text{loc}}[\phi_i^*, \phi_i], \quad (90)$$

which is precisely Eq. (169).

Near the MI–SF transition, ϕ is small and slowly varying. A cumulant (linked-cluster) expansion of $-\ln \mathcal{Z}_{\text{loc}}$ yields a derivative-expanded continuum action

$$S_{\text{EFT}}[\phi^*, \phi] = \int_0^\beta d\tau \int d^d r [u \phi^* \partial_\tau \phi + v |\partial_\tau \phi|^2 + w |\nabla \phi|^2 - a |\phi|^2 + b |\phi|^4 + \dots], \quad (91)$$

namely Eq. (200). The coefficients are determined by (i) the small- (k, ω) expansion of the quadratic kernel $\mathcal{K}(k, i\omega_n) = t(k)^{-1} - G(i\omega_n)$ (Eq. (191)), and (ii) local atomic-limit correlators (e.g. the connected 4-point function for b).

5.2 Ward identity: $U(1)$ symmetry constraint between u and a

From microscopic $U(1)$ to “ μ as a background field”.

The Bose–Hubbard Hamiltonian conserves total particle number $\hat{N} = \sum_i \hat{n}_i$, hence has a global $U(1)$ symmetry $\hat{b}_i \rightarrow e^{i\theta} \hat{b}_i$. In the coherent-state path integral this becomes $b_i(\tau) \rightarrow e^{i\theta(\tau)} b_i(\tau)$, $b_i^*(\tau) \rightarrow e^{-i\theta(\tau)} b_i^*(\tau)$, with θ allowed to depend on τ (global in space, local in imaginary time). The Berry term⁹ transforms as

$$b_i^* \partial_\tau b_i \longrightarrow b_i^* \partial_\tau b_i + i(\partial_\tau \theta) |b_i|^2, \quad (92)$$

which brings an extra $|b_i|^2$ term. Therefore, the microscopic action remains invariant only if the chemical potential is shifted simultaneously as

$$\mu \longrightarrow \mu + i\partial_\tau \theta, \quad (93)$$

so μ plays the role of a background temporal gauge field.

Derivation of the Ward Identity $u = \partial_\mu a..$

The EFT must inherit the same background-field symmetry. Under $\phi \rightarrow e^{i\theta(\tau)} \phi$, one finds

$$\phi^* \partial_\tau \phi \longrightarrow \phi^* \partial_\tau \phi + i(\partial_\tau \theta) |\phi|^2. \quad (94)$$

Plug in (91), and one finds the first-order temporal term contributes

$$\delta S_u = \int d\tau d^d r i u (\partial_\tau \theta) |\phi|^2. \quad (95)$$

On the other hand, background-field invariance demands that the EFT responds to $\mu \rightarrow \mu + i\partial_\tau \theta$. Since $a = a(\mu)$, the mass term changes as

$$-a(\mu) |\phi|^2 \longrightarrow -a(\mu + i\partial_\tau \theta) |\phi|^2 \simeq -a(\mu) |\phi|^2 - \frac{\partial a}{\partial \mu} i(\partial_\tau \theta) |\phi|^2, \quad (96)$$

⁹The Berry term refers to the first term in (87)

so

$$\delta S_a = - \int d\tau d^d r \frac{\partial a}{\partial \mu} i(\partial_\tau \theta) |\phi|^2. \quad (97)$$

Requiring $\delta S_u + \delta S_a = 0$ for arbitrary $\theta(\tau)$ gives the constraint

$$u = \frac{\partial a}{\partial \mu}.$$

(98)

Relation to the QFT ‘‘Ward identity’’. Eq. (98) is the EFT version of a Ward identity: coupling the conserved $U(1)$ current to a background gauge field A_τ and demanding invariance under $A_\tau \rightarrow A_\tau + \partial_\tau \theta$ forces specific relations among EFT coefficients. Here $A_\tau \equiv \mu$, and the identity ties the coefficient of $\phi^* \partial_\tau \phi$ to the μ -dependence of the mass term.

5.3 Computing u from $a(\mu)$: the particle–hole symmetric line

Mean-field $a(\mu)$ and explicit u . Using the mean-field (Gaussian) result from Appendix C,

$$a(\mu) = \frac{n_0 + 1}{Un_0 - \mu} + \frac{n_0}{\mu - U(n_0 - 1)} - \frac{1}{Z}, \quad (99)$$

the Ward identity (98) gives

$$u(\mu) = \frac{\partial a}{\partial \mu} = \frac{n_0 + 1}{(Un_0 - \mu)^2} - \frac{n_0}{(\mu - U(n_0 - 1))^2}. \quad (100)$$

Writing $E_p \equiv Un_0 - \mu$ and $E_h \equiv \mu - U(n_0 - 1)$, one has

$$u = 0 \iff \frac{n_0 + 1}{E_p^2} = \frac{n_0}{E_h^2} \iff \frac{E_h}{E_p} = \sqrt{\frac{n_0}{n_0 + 1}}. \quad (101)$$

Thus $u = 0$ occurs where particle and hole processes are comparably important. For large filling $n_0 \gg 1$, $\sqrt{\frac{n_0}{n_0 + 1}} \simeq 1$, so $u \simeq 0$ is well approximated by $E_p \simeq E_h$, i.e. the particle–hole symmetric line near the lobe tip.

5.4 Emergent Lorentz symmetry: why $u \neq 0$ is nonrelativistic but $u = 0$ is relativistic

Generic case $u \neq 0$: first-order time derivative \Rightarrow nonrelativistic scaling.

At quadratic order, the kernel is schematically

$$S^{(2)} \sim \int d\tau d^d r [u \phi^* \partial_\tau \phi + w |\nabla \phi|^2 - a |\phi|^2]. \quad (102)$$

In Fourier space this gives $S^{(2)} \sim \sum_{k,\omega} \phi^*(\mathbf{k}, \omega) [-iu\omega + wk^2 - a] \phi(\mathbf{k}, \omega)$, so the dispersion scales as $\omega \sim k^2$. Equivalently, under coarse graining $\mathbf{r} \rightarrow s\mathbf{r}$ one needs $\tau \rightarrow s^z \tau$ with

$$z = 2, \quad (103)$$

which is the hallmark of a nonrelativistic critical theory.

Special line $u = 0$: second-order time derivative \Rightarrow emergent Lorentz invariance.

When $u = 0$, the leading temporal term is $v |\partial_\tau \phi|^2$, and the quadratic action becomes

$$S^{(2)} \sim \int d\tau d^d r [v |\partial_\tau \phi|^2 + w |\nabla \phi|^2 - a |\phi|^2]. \quad (104)$$

Define an effective “light velocity” $c \equiv \sqrt{w/v}$ and rescale time as $\tilde{\tau} \equiv c\tau$. Then the derivative part is isotropic:

$$v|\partial_\tau\phi|^2 + w|\nabla\phi|^2 = w(|\partial_{\tilde{\tau}}\phi|^2 + |\nabla\phi|^2), \quad (105)$$

which is the Euclidean form of a relativistic ($z = 1$) scalar field theory. This Lorentz symmetry is not microscopic; it emerges at low energies on the $u = 0$ line.

5.5 Distinct critical behavior: Relativistic vs Nonrelativistic

(I) Mott Phase $a < 0$.

We first discuss the Mott side ($a < 0$). The quadratic potential is $+|a||\phi|^2$, and the excitation gap is read off from the quadratic kernel.

- *Relativistic case ($u = 0$)*.

Fourier transforming,

$$S^{(2)} \sim \sum_{k,\omega} [v\omega^2 + wk^2 + |a|] |\phi(\mathbf{k}, \omega)|^2. \quad (106)$$

After analytic continuation $i\omega \rightarrow \omega$, the pole condition is $v\omega^2 = wk^2 + |a|$, i.e.

$$\omega^2(k) = c^2k^2 + \Delta^2, \quad c^2 = \frac{w}{v}, \quad \Delta^2 = \frac{|a|}{v}. \quad (107)$$

Hence the gap scales as

$$\boxed{\Delta \propto \sqrt{|a|}, \quad (u = 0, z = 1).} \quad (108)$$

This is the standard statement that in a relativistic theory the mass term is $m^2 \sim |a|$, so the physical gap is $m \sim \sqrt{|a|}$.

- *Nonrelativistic case ($u \neq 0$)*.

Now the quadratic kernel is

$$S^{(2)} \sim \sum_{k,\omega} [-iu\omega + wk^2 + |a|] |\phi(\mathbf{k}, \omega)|^2, \quad (109)$$

giving (after analytic continuation) a dispersion of the form

$$\omega(k) \sim \frac{wk^2 + |a|}{u}, \quad \Rightarrow \quad \boxed{\Delta \propto |a|, \quad (u \neq 0, z = 2).} \quad (110)$$

(II) Superfluid Phase $a > 0$.

When $a > 0$, the potential $-a|\phi|^2 + b|\phi|^4$ is minimized at a nonzero condensate amplitude

$$|\phi_0|^2 = \frac{a}{2b}, \quad (111)$$

so we parametrize fluctuations as $\phi = (\phi_0 + \delta\rho)e^{i\theta}$. To quadratic order, the phase field θ is gapless (Goldstone mode) while the amplitude fluctuation $\delta\rho$ is massive (Higgs mode). In the relativistic case ($u = 0$),

$$\omega_G(k) = ck, \quad \omega_H(k) = \sqrt{c^2k^2 + \Delta_H^2}, \quad \Delta_H^2 \sim \frac{a}{v}, \quad (112)$$

so the Higgs gap scales as $\Delta_H \propto \sqrt{a}$ near criticality, consistent with the interpretation of $|a|$ as a relativistic mass-squared.

Away from particle-hole symmetry ($u \neq 0$), the phase mode remains gapless but the temporal structure is nonrelativistic ($z = 2$), and the precise Higgs-gap scaling is not protected by Lorentz invariance and $\Delta \propto a$. See Appendix A for more discussion on the non-relativistic case.

Two distinct critical behaviors in the BHM (Mean-field scaling).

Spatial correlations are controlled by $wk^2 + |a|$, so $\xi \sim \sqrt{w/|a|}$ and $\nu = 1/2$ in both cases at mean-field level. The *dynamical* scaling differs:

- Away from particle-hole symmetry ($u \neq 0$): $z = 2$, $\Delta \propto |a|$, hence $z\nu = 1$.
- On the particle-hole symmetric line ($u = 0$): $z = 1$, $\Delta \propto \sqrt{|a|}$, hence $z\nu = 1/2$.

A Critical scaling of the gap (non-relativistic, away from p-h symmetric point)

This appendix provides a detailed derivation of the (mean-field) *linear* critical closing of the relevant low-energy scale in the vicinity of the MI-SF transition *away from the particle-hole symmetric point* (i.e. away from the Mott-lobe tip). In this non-relativistic regime the transition is density-driven and is expected to obey the scaling form

$$\Delta \sim |g - g_c|^{z\nu}, \quad (113)$$

with dynamic exponent $z = 2$; our explicit derivations below yield $z\nu = 1$ and hence $\nu = 1/2$.

A.1 Mott-insulator side: strong-coupling gaps and linear closing

In the leading strong-coupling (atomic-limit) treatment, the lowest particle/hole excitation gaps in the n_0 -th Mott lobe are¹⁰

$$\Delta_p(J) = Un_0 - \mu - ZJ(n_0 + 1), \quad (114)$$

$$\Delta_h(J) = \mu - U(n_0 - 1) - ZJn_0, \quad (115)$$

and the smallest gap controlling the MI stability is

$$\Delta_-(J) \equiv \min\{\Delta_p(J), \Delta_h(J)\}, \quad (116)$$

cf. Eq. (52).

Particle-driven boundary (upper boundary). Fix μ within the n_0 -th lobe and consider approaching the *upper* boundary where the particle gap closes first. The critical point $J = J_c^{(p)}$ is defined by $\Delta_p(J_c^{(p)}) = 0$, i.e.

$$Un_0 - \mu - ZJ_c^{(p)}(n_0 + 1) = 0 \implies J_c^{(p)} = \frac{Un_0 - \mu}{Z(n_0 + 1)}. \quad (117)$$

Then for J near $J_c^{(p)}$,

$$\Delta_p(J) = Un_0 - \mu - ZJ(n_0 + 1) = Z(n_0 + 1)(J_c^{(p)} - J), \quad (118)$$

so the minimum gap on the MI side behaves as

$$\Delta_-(J) = \Delta_p(J) \propto |J - J_c^{(p)}|. \quad (119)$$

¹⁰In dimensionless variables $x \equiv J/U$ and $y \equiv \mu/U$, one may write $\Delta_p/U = n_0 - y - Zx(n_0 + 1)$ and $\Delta_h/U = y - (n_0 - 1) - Zxn_0$.

Hole-driven boundary (lower boundary). Similarly, approaching the *lower* boundary where the hole gap closes first, the critical point $J = J_c^{(h)}$ is defined by $\Delta_h(J_c^{(h)}) = 0$, i.e.

$$\mu - U(n_0 - 1) - ZJ_c^{(h)}n_0 = 0 \implies J_c^{(h)} = \frac{\mu - U(n_0 - 1)}{Zn_0}. \quad (120)$$

Near $J_c^{(h)}$,

$$\Delta_h(J) = \mu - U(n_0 - 1) - ZJn_0 = Zn_0(J_c^{(h)} - J), \quad (121)$$

hence

$$\Delta_{-}(J) = \Delta_h(J) \propto |J - J_c^{(h)}|. \quad (122)$$

Remark on the lobe tip. At the lobe tip the upper and lower boundaries meet; within this leading-order strong-coupling picture one finds that both Δ_p and Δ_h vanish at the same J_{\star} , but with *different* linear coefficients, $\Delta_p \sim Z(n_0 + 1)(J_{\star} - J)$ and $\Delta_h \sim Zn_0(J_{\star} - J)$. This mismatch indicates that the tip is a special point where additional subtleties (not captured by the leading $O(J/U)$ treatment) may become important; in particular, the true critical theory at the tip is relativistic ($z = 1$), while the present appendix focuses on the non-relativistic regime away from the tip.

A.2 Superfluid side: Landau expansion and linear scaling of the low-energy scale

We now analyze the SF side using the Landau expansion (mean-field) energy density per site

$$\mathcal{E}(\phi) = \mathcal{E}_0 - a|\phi|^2 + b|\phi|^4 + \dots, \quad (b > 0), \quad (123)$$

(i) Linear expansion of $a(J)$ near J_c

We start from the explicit mean-field expression (see Eq. (74))

$$a = \frac{n_0 + 1}{Un_0 - \mu} + \frac{n_0}{\mu - U(n_0 - 1)} - \frac{1}{ZJ}. \quad (124)$$

For fixed μ , define

$$A(\mu) \equiv \frac{n_0 + 1}{Un_0 - \mu} + \frac{n_0}{\mu - U(n_0 - 1)}, \quad (125)$$

so that $a(J) = A(\mu) - \frac{1}{ZJ}$. The critical line is determined by $a(J_c) = 0$, namely

$$A(\mu) = \frac{1}{ZJ_c}. \quad (126)$$

Let $J = J_c + \delta J$ and expand

$$\frac{1}{J} = \frac{1}{J_c + \delta J} = \frac{1}{J_c} \frac{1}{1 + \delta J/J_c} = \frac{1}{J_c} - \frac{\delta J}{J_c^2} + O(\delta J^2). \quad (127)$$

Using (126), we obtain *strictly*

$$a(J) = A - \frac{1}{ZJ} = \frac{1}{ZJ_c} - \frac{1}{Z} \left(\frac{1}{J_c} - \frac{\delta J}{J_c^2} + O(\delta J^2) \right) = \frac{\delta J}{ZJ_c^2} + O(\delta J^2), \quad (128)$$

i.e.

$$a(J) = \frac{J - J_c}{ZJ_c^2} + O((J - J_c)^2), \quad \Rightarrow \quad |a| \propto |J - J_c|. \quad (129)$$

One can also re-write (129) in a dimensionless form.¹¹

¹¹Writing in dimensionless form $x \equiv J/U$ gives the equivalent expansion

$$a(J) = \frac{x - x_c}{ZUx_c^2} + O((x - x_c)^2), \quad x_c = \frac{J_c}{U}.$$

(ii) Expansion around the SF minima

On the SF side one has $a > 0$, and Eq. (123) yields the familiar ‘‘Mexican-hat’’ energy landscape. Around a local minimum, there are two normal modes, as is standard in a $U(1)$ -symmetry-breaking setting: the *angular* (phase) fluctuation is the Goldstone mode and hence corresponds to a gapless excitation, while the *radial* (amplitude) fluctuation is gapped. The latter allows one to extract a characteristic low-energy scale, denoted by Δ_+ . To compute Δ_+ explicitly, we fix the overall phase of ϕ (gauge-fix) and take ϕ to be real:

Minimizing $\mathcal{E}(\phi)$ yields

$$\frac{d\mathcal{E}}{d\phi} = -2a\phi + 4b\phi^3 = 0 \quad \Rightarrow \quad \phi = \pm\phi_0, \quad \phi_0^2 = \frac{a}{2b}. \quad (130)$$

Expand about one minimum, $\phi = \phi_0 + \delta\phi$. The second derivative at the minimum is

$$\left. \frac{d^2\mathcal{E}}{d\phi^2} \right|_{\phi_0} = -2a + 12b\phi_0^2 = -2a + 12b \cdot \frac{a}{2b} = 4a, \quad (131)$$

and hence the Landau energy to quadratic order is

$$\mathcal{E}(\phi_0 + \delta\phi) = \mathcal{E}(\phi_0) + \frac{1}{2}(4a)(\delta\phi)^2 + \dots = \mathcal{E}(\phi_0) + 2a(\delta\phi)^2 + \dots. \quad (132)$$

Therefore, *the curvature (local stiffness) around the SF minimum is proportional to a .*

(iii) Identification with the SF low-energy scale and critical exponent

Away from the particle-hole symmetric point the effective critical dynamics is non-relativistic (density-driven) with $z = 2$. In such a theory the relevant low-energy scale on the SF side, denoted Δ_+ in the main text, is controlled by the local stiffness/curvature around the minimum, hence

$$\Delta_+ \propto a. \quad (133)$$

Combining (133) with the linear expansion (129) gives

$$\Delta_+ \propto a \propto |J - J_c| \propto \left| \frac{J}{U} - \left(\frac{J}{U} \right)_c \right|, \quad (134)$$

i.e. the low-energy scale vanishes *linearly* at the transition in the non-relativistic regime away from the tip.

A.3 Critical Gap Scaling

Now we have derived that on both the MI side and the SF side, Δ scales linearly with $|g - g_c|$, where $g \equiv J/U$. Comparing with $\Delta \sim |g - g_c|^{z\nu}$ yields

$$z\nu = 1. \quad (135)$$

Since $z = 2$ in the non-relativistic universality class, one finds $\nu = 1/2$ at mean-field level.

B Coherent-state path integral: a self-contained derivation

Conceptually, there are two common “routes” to a path integral: (i) a coordinate/momentum (x - p) representation, which is closest to the *first-quantized* picture of particle trajectories; (ii) a coherent-state representation, which is most natural in the *second-quantized* language, where the Hamiltonian is already written in terms of creation/annihilation operators (or field operators). For lattice bosons (and more generally for many-body Hamiltonians expressed in \hat{b}, \hat{b}^\dagger), the coherent-state route is typically more direct and avoids cumbersome operator ordering issues that would arise in an x - p formulation.

B.1 Bosonic coherent states: definitions and identities

Consider a single bosonic mode with $[\hat{b}, \hat{b}^\dagger] = 1$. A coherent state $|\alpha\rangle$ is defined as an eigenstate of the annihilation operator, parametrized by $\alpha \in \mathbb{C}$,

$$\hat{b}|\alpha\rangle = \alpha|\alpha\rangle, \quad \alpha \in \mathbb{C}. \quad (136)$$

It admits the explicit construction

$$|\alpha\rangle = e^{-|\alpha|^2/2} e^{\alpha\hat{b}^\dagger} |0\rangle, \quad (137)$$

where $|0\rangle$ is the vacuum. Coherent states are **complete** and obey the resolution of identity¹²:

$$\mathbf{1} = \int \frac{d^2\alpha}{\pi} |\alpha\rangle\langle\alpha|. \quad (138)$$

They are **non-orthogonal**:

$$\langle\alpha'|\alpha\rangle = \exp\left(-\frac{1}{2}|\alpha'|^2 - \frac{1}{2}|\alpha|^2 + \alpha'^*\alpha\right). \quad (139)$$

When calculating matrix elements, the relation

$$\langle\alpha'|\hat{b}^\dagger = \alpha'^*\langle\alpha'|, \quad \hat{b}|\alpha\rangle = \alpha|\alpha\rangle, \quad (140)$$

is very useful to “kill” operator insertions, and turn operators to *c*-numbers.

Multi-mode generalization. For many bosonic modes labeled by i (lattice sites, orbitals, . . .), define $|\{\alpha_i\}\rangle \equiv \bigotimes_i |\alpha_i\rangle$. Then the resolution of identity becomes

$$\mathbf{1} = \int \prod_i \frac{d^2\alpha_i}{\pi} |\{\alpha_i\}\rangle\langle\{\alpha_i\}|, \quad (141)$$

and the overlap (139) factorizes into a product over modes.

B.2 From operators to a path integral: Trotter slicing

We work in Euclidean time. The partition function at inverse temperature β is

$$\mathcal{Z} = \text{Tr } e^{-\beta\hat{H}}. \quad (142)$$

The Euclidean formulation is convenient because $e^{-\beta\hat{H}}$ plays the role of an “imaginary-time evolution” operator. Introduce a time step $\Delta\tau = \beta/M$ and apply the Trotter decomposition,

$$e^{-\beta\hat{H}} = \left(e^{-\Delta\tau\hat{H}}\right)^M \quad (M \rightarrow \infty). \quad (143)$$

At this stage no basis has been chosen. The next step is to insert resolutions of identity between factors of $e^{-\Delta\tau\hat{H}}$. In the coherent-state approach, we insert (141).

¹²Here $d^2\alpha$ means integrating over the whole complex plane, *i.e.* $d^2\alpha \equiv d(\text{Re}(\alpha))d(\text{Im}(\alpha))$. Actually Coherent states are *overcomplete*.

Euclidean propagator as a “generalized partition function”

For two coherent states $|\alpha_i\rangle$ and $|\alpha_f\rangle$, the Euclidean propagator

$$K(\alpha_f^*, \alpha_i; \beta) \equiv \langle \alpha_f | e^{-\beta \hat{H}} | \alpha_i \rangle$$

has the same path-integral structure as \mathcal{Z} , but with *fixed boundary conditions* at $\tau = 0, \beta$ instead of a trace. The partition function is obtained by taking the trace, which corresponds to integrating over equal initial&final coherent states and yields periodic boundary conditions for bosons.

B.3 Derivation of the coherent-state path integral

For clarity, we first present the one-mode derivation and then state the multi-mode result.

Step 1: short-time matrix elements and normal ordering

Insert $M - 1$ coherent-state resolutions of identity between Trotter factors (143). Denote the discrete (imaginary) time slices by $m = 0, 1, \dots, M$, with $\tau_m = m\Delta\tau$. For a one-mode system,

$$\mathcal{Z} = \int \prod_{m=0}^{M-1} \frac{d^2 \alpha_m}{\pi} \prod_{m=0}^{M-1} \langle \alpha_{m+1} | e^{-\Delta\tau \hat{H}} | \alpha_m \rangle, \quad \alpha_M \equiv \alpha_0, \quad (144)$$

where the identification $\alpha_M = \alpha_0$ implements the trace (periodic boundary condition).

To evaluate the short-time matrix element, expand for small $\Delta\tau$,

$$e^{-\Delta\tau \hat{H}} = 1 - \Delta\tau \hat{H} + O(\Delta\tau^2).$$

Assume \hat{H} is written in *normal-ordered* form, $\hat{H} =: H(\hat{b}^\dagger, \hat{b}) :$, then the coherent-state matrix element factorizes:

$$\langle \alpha_{m+1} | \hat{H} | \alpha_m \rangle = H(\alpha_{m+1}^*, \alpha_m) \langle \alpha_{m+1} | \alpha_m \rangle, \quad (145)$$

and hence

$$\boxed{\langle \alpha_{m+1} | e^{-\Delta\tau \hat{H}} | \alpha_m \rangle = \langle \alpha_{m+1} | \alpha_m \rangle \exp \left[-\Delta\tau H(\alpha_{m+1}^*, \alpha_m) \right] + O(\Delta\tau^2)}. \quad (146)$$

The indices $m, m + 1$ emphasize that α_m is the c-number field living on the discrete imaginary-time lattice¹³.

What does “normal ordered” mean?

An operator expression is normal ordered if all creation operators \hat{b}^\dagger appear to the left of all annihilation operators \hat{b} . For bosons, normal ordering is achieved by repeatedly commuting \hat{b} past \hat{b}^\dagger using $[\hat{b}, \hat{b}^\dagger] = 1$. In normal-ordered form, coherent-state matrix elements are simple because \hat{b} acting on $|\alpha\rangle$ yields α , while \hat{b}^\dagger acting on $\langle\alpha'|$ yields α'^* , cf. (140).

Step 2: collecting the exponent and “killing” operators

Substituting (146) into (144), we obtain a product of purely c-number factors:

$$\mathcal{Z} \propto \int \prod_{m=0}^{M-1} \frac{d^2 \alpha_m}{\pi} \exp \left\{ \sum_{m=0}^{M-1} \ln \langle \alpha_{m+1} | \alpha_m \rangle - \Delta\tau \sum_{m=0}^{M-1} H(\alpha_{m+1}^*, \alpha_m) \right\}, \quad (147)$$

¹³Later m will be replaced by continuous τ

where \propto hides an overall normalization constant. At this stage, *all operators have disappeared*: the only remaining objects are complex numbers α_m, α_m^* . In particular, there is no further concern about commutation relations. This is the magic of path integral, where all the information of operator algebras are encoded in the integral formalism, and all that is left are merely numbers.

Using the overlap (139),

$$\ln\langle\alpha_{m+1}|\alpha_m\rangle = -\frac{1}{2}|\alpha_{m+1}|^2 - \frac{1}{2}|\alpha_m|^2 + \alpha_{m+1}^*\alpha_m. \quad (148)$$

A convenient rearrangement of the sum is¹⁴

$$\sum_{m=0}^{M-1} (\alpha_{m+1}^*\alpha_m - \alpha_m^*\alpha_m) = - \sum_{m=1}^{M-1} \alpha_m^*(\alpha_m - \alpha_{m-1}) + (\alpha_M^*\alpha_{M-1} - \alpha_0^*\alpha_0), \quad (149)$$

where the last term correspond to a boundary term. Specifically, we are using the periodic boundary condition $\alpha_M = \alpha_0$. Usually we denote $\alpha_{-1} \equiv \alpha_{M-1}$, and rewrite Eq. (149) as:

$$\sum_{m=0}^{M-1} (\alpha_{m+1}^*\alpha_m - \alpha_m^*\alpha_m) = - \sum_{m=0}^{M-1} \alpha_m^*(\alpha_m - \alpha_{m-1}), \quad (\alpha_M = \alpha_0, \alpha_{-1} = \alpha_{M-1}). \quad (150)$$

Step 3: continuum limit and the Euclidean action

In the limit $M \rightarrow \infty$, we interpret $\alpha_m \equiv \alpha(\tau_m)$ as samples of a smooth field $\alpha(\tau)$. Then

$$\alpha_m - \alpha_{m-1} = \Delta\tau \partial_\tau \alpha(\tau_m) + O(\Delta\tau^2), \quad (151)$$

and the discrete sum becomes

$$\sum_{m=0}^{M-1} \alpha_m^*(\alpha_m - \alpha_{m-1}) \longrightarrow \int_0^\beta d\tau \alpha^*(\tau) \partial_\tau \alpha(\tau). \quad (152)$$

Similarly, the Riemann sum $\Delta\tau \sum_m H(\alpha_{m+1}^*, \alpha_m)$ tends to $\int_0^\beta d\tau H(\alpha^*(\tau), \alpha(\tau))$ up to the chosen discretization convention (left/right endpoints differ by higher-order terms in $\Delta\tau$).

Therefore, the bosonic partition function admits the coherent-state path-integral representation

$$\mathcal{Z} = \int_{\text{PBC}} \mathcal{D}[\alpha^*, \alpha] \exp\left\{- \int_0^\beta d\tau [\alpha^*(\tau) \partial_\tau \alpha(\tau) + H(\alpha^*(\tau), \alpha(\tau))]\right\}, \quad (153)$$

where “PBC” denotes periodic boundary conditions $\alpha(\beta) = \alpha(0)$ required by the trace.

Propagator version and boundary conditions

For the Euclidean propagator $K(\alpha_f^*, \alpha_i; \beta) = \langle \alpha_f | e^{-\beta \hat{H}} | \alpha_i \rangle$, the path integral has the same action as (153), but the fields obey fixed boundary conditions $\alpha(0) = \alpha_i$, $\alpha(\beta) = \alpha_f$ rather than periodicity. Endpoint terms that vanish for \mathcal{Z} remain explicit for K .

B.4 Many-body generalization and the Bose–Hubbard example

For a set of bosonic modes b_i , replace $\alpha \rightarrow \{\alpha_i\}$ in (153). The fields $\alpha_i(\tau)$ depend on imaginary time, so the path integral is naturally interpreted as a $(d+1)$ -dimensional classical statistical

¹⁴This corresponds to a discrete *integration-by-part*.

field theory (with τ playing the role of an extra dimension). The general coherent-state path integral reads

$$\mathcal{Z} = \int_{\text{PBC}} \mathcal{D}[\alpha^*, \alpha] \exp \left\{ - \int_0^\beta d\tau \left[\sum_i \alpha_i^*(\tau) \partial_\tau \alpha_i(\tau) + H(\{\alpha_i^*(\tau)\}, \{\alpha_i(\tau)\}) \right] \right\}. \quad (154)$$

and the action S reads

$$S[\alpha^*, \alpha] = \int_0^\beta d\tau \left[\sum_i \alpha_i^*(\tau) \partial_\tau \alpha_i(\tau) + H(\{\alpha_i^*(\tau)\}, \{\alpha_i(\tau)\}) \right]. \quad (155)$$

■ Example: the Bose–Hubbard model

Consider the Bose–Hubbard Hamiltonian

$$\hat{H} = -J \sum_{\langle ij \rangle} (\hat{b}_i^\dagger \hat{b}_j + \text{h.c.}) + \sum_i \left[\frac{U}{2} \hat{n}_i(\hat{n}_i - 1) - \mu \hat{n}_i \right], \quad \hat{n}_i = \hat{b}_i^\dagger \hat{b}_i. \quad (156)$$

This Hamiltonian is already normal ordered: $\hat{b}_i^\dagger \hat{b}_j$ has \hat{b}^\dagger to the left of \hat{b} , and $\hat{n}_i(\hat{n}_i - 1)$ can be written as $\hat{b}_i^\dagger \hat{b}_i^\dagger \hat{b}_i \hat{b}_i$ with all creation operators on the left. Therefore, we may directly apply (154) by replacing $\hat{b}_i, \hat{b}_i^\dagger$ with c-numbers $b_i(\tau), b_i^*(\tau)$. The Euclidean action becomes

$$S[b^*, b] = \int_0^\beta d\tau \left[\sum_i b_i^*(\tau) \partial_\tau b_i(\tau) - J \sum_{\langle ij \rangle} (b_i^*(\tau) b_j(\tau) + \text{c.c.}) + \sum_i \left(\frac{U}{2} |b_i(\tau)|^4 - \mu |b_i(\tau)|^2 \right) \right], \quad (157)$$

and hence

$$\mathcal{Z}_{\text{BHM}} = \int_{\text{PBC}} \mathcal{D}[b^*, b] e^{-S[b^*, b]}, \quad b_i(\beta) = b_i(0). \quad (158)$$

C From coherent-state path integral to a long-wavelength effective action

Here we derive a continuum long-wavelength effective action for the superfluid order parameter starting from the coherent-state path integral of a lattice boson Hamiltonian. The logic is deliberately explicit: we first obtain an *exact* (but generally nonlocal) effective action $S_{\text{eff}}[\phi]$ by a Hubbard–Stratonovich (HS) decoupling of the hopping term and integrating out the microscopic boson fields. Only *afterwards* do we perform a low-frequency/long-wavelength expansion to arrive at the familiar derivative-expanded effective field theory (EFT).

A. Starting point: coherent-state path integral on the lattice

Consider a bosonic lattice model (e.g. the Bose–Hubbard model). The coherent-state path integral representation of the partition function reads

$$\mathcal{Z} = \int_{\text{PBC}} \mathcal{D}[b^*, b] e^{-S[b^*, b]}, \quad b_i(\beta) = b_i(0), \quad (159)$$

with Euclidean action of the generic form

$$S[b^*, b] = S_{\text{loc}}[b^*, b] - \int_0^\beta d\tau \sum_{ij} b_i^*(\tau) t_{ij} b_j(\tau). \quad (160)$$

Here

- $b_i(\tau) \in \mathbb{C}$ is a c-number field living on lattice site i and (imaginary) time $\tau \in [0, \beta]$;
- S_{loc} is *strictly on-site* (no coupling between different sites), typically containing the Berry-phase term and the on-site interaction/chemical potential. Typically one can write

$$S_{\text{loc}} = \sum_i S_{0,i} \quad , \quad S_{0,i} \text{ is the local action on the } i\text{'th site;} \quad (161)$$

- t_{ij} is the hopping matrix (for nearest-neighbor hopping on a regular lattice, $t_{ij} = J$ for $\langle ij \rangle$, and $t_{ij} = 0$ otherwise).

Concrete example: Bose–Hubbard model. For $\hat{H} = -J \sum_{\langle ij \rangle} (\hat{b}_i^\dagger \hat{b}_j + \text{h.c.}) + \sum_i \left[\frac{U}{2} \hat{n}_i (\hat{n}_i - 1) - \mu \hat{n}_i \right]$, the corresponding Euclidean action is

$$S_{\text{BHM}}[b^*, b] = \int_0^\beta d\tau \left[\sum_i b_i^*(\tau) \partial_\tau b_i(\tau) - J \sum_{\langle ij \rangle} (b_i^*(\tau) b_j(\tau) + \text{c.c.}) + \sum_i \left(\frac{U}{2} |b_i(\tau)|^4 - \mu |b_i(\tau)|^2 \right) \right]. \quad (162)$$

What is the goal of the “long-wavelength EFT”?

Near the MI–SF transition, the low-energy physics is governed by a slowly varying complex order-parameter field $\phi(r, \tau)$ describing phase coherence. We aim to derive an effective action for ϕ , then expand it for small frequencies and small momenta to obtain a continuum theory with a few coefficients (“Landau + derivatives”):

$$S_{\text{EFT}} = \int d\tau d^d r \left[u \phi^* \partial_\tau \phi + v |\partial_\tau \phi|^2 + w |\nabla \phi|^2 - a |\phi|^2 + b |\phi|^4 + \dots \right].$$

Importantly, we will *not* assume this form at the beginning; we derive it by controlled expansions.

B. Introducing the order-parameter field ϕ via HS decoupling

The only nonlocal piece in (160) is the hopping term, which is bilinear in b :

$$S_J[b^*, b] \equiv - \int_0^\beta d\tau \sum_{ij} b_i^*(\tau) t_{ij} b_j(\tau). \quad (163)$$

Our goal is to transform the partition function into an *on-site* form. The key technique will be the *Hubbard–Stratonovich transformation*.

In the Boltzmann weight e^{-S} , the action S appears as

$$e^{-S_J} = e^{\int d\tau b^\dagger t b}$$

, where $b^\dagger t b \equiv \sum_{ij} b_i^* t_{ij} b_j$. We now decouple this quadratic form by introducing an auxiliary complex field $\phi_i(\tau)$ using a Hubbard–Stratonovich identity. Refer to the following box if you are not familiar with Hubbard–Stratonovich transformation.

Hubbard–Stratonovich identity (Complex number, finite-dimensional version)

Let $b \in \mathbb{C}^N$ be a complex column vector, and let $t \in \mathbb{C}^{N \times N}$ be an invertible matrix (typically taken Hermitian in applications). Introduce an auxiliary complex field $\phi \in \mathbb{C}^N$ with independent integration variables $\{\phi_i, \phi_i^*\}_{i=1}^N$. Then the following Hubbard–Stratonovich

identity holds:

$$\exp(b^\dagger t b) \propto \int d\phi^* d\phi \exp(-\phi^\dagger t^{-1} \phi + \phi^\dagger b + b^\dagger \phi), \quad (164)$$

where $d\phi^* d\phi \equiv \prod_{i=1}^N d\phi_i^* d\phi_i$, and the proportionality constant is a field-independent normalization.

Proof.

The exponent can be rewritten as

$$-\phi^\dagger t^{-1} \phi + \phi^\dagger b + b^\dagger \phi = -(\phi - tb)^\dagger t^{-1} (\phi - tb) + b^\dagger tb.$$

Therefore,

$$\int d\phi^* d\phi e^{-\phi^\dagger t^{-1} \phi + \phi^\dagger b + b^\dagger \phi} = \int d\phi^* d\phi e^{-(\phi - tb)^\dagger t^{-1} (\phi - tb)} \times e^{b^\dagger tb}.$$

The first factor is independent of b : by the translation $\phi \mapsto \phi + tb$, it becomes a pure Gaussian normalization constant. Hence the integral is proportional to $e^{b^\dagger tb}$, which proves the identity.

From (164), one can use the H-S identity to a integral. Consider

$$\exp\left\{ + \int_0^\beta d\tau b^\dagger(\tau) t b(\tau) \right\} = \prod_\tau \exp\left\{ + b^\dagger(\tau) t b(\tau) d\tau \right\}.$$

Replacing each $\exp\{b^\dagger(\tau) t b(\tau) d\tau\}$ by the ϕ -integral in (164), and multiplying them together, we get:

$$\begin{aligned} \exp\left\{ \int_0^\beta d\tau b^\dagger(\tau) t b(\tau) \right\} &= \prod_\tau \int d\phi^*(\tau) d\phi(\tau) \exp\left[-\phi^\dagger(\tau) t^{-1} \phi(\tau) + \phi^\dagger(\tau) b(\tau) + b^\dagger(\tau) \phi(\tau) \right] \\ &= \int \mathcal{D}[\phi^*, \phi] \exp\left\{ \int_0^\beta d\tau \left[-\phi^\dagger(\tau) t^{-1} \phi(\tau) + \phi^\dagger(\tau) b(\tau) + b^\dagger(\tau) \phi(\tau) \right] \right\}, \end{aligned} \quad (165)$$

where $\mathcal{D}[\phi^*, \phi] \equiv \prod_{\tau,i} d\phi_i^*(\tau) d\phi_i(\tau)$.

Conditions of validity. The algebraic completion-of-square step only requires that t be invertible. For the ϕ -integral to converge as an ordinary Gaussian integral, one needs the quadratic form $\phi^\dagger t^{-1} \phi$ to have a positive real part (e.g. t Hermitian positive definite). In lattice applications where t may be indefinite, the identity is commonly used as a formal/analytic-continuation manipulation (or with an implicit contour rotation / regulator that ensures convergence). In a coherent-state path integral, the same identity is applied independently at each imaginary time τ .

Applying the HS identity (165) to the hopping factor yields

$$\exp\left\{ \int_0^\beta d\tau \sum_{ij} b_i^*(\tau) t_{ij} b_j(\tau) \right\} \propto \int \mathcal{D}[\phi^*, \phi] \exp\left\{ - \int_0^\beta d\tau \sum_{ij} \phi_i^*(\tau) (t^{-1})_{ij} \phi_j(\tau) + \int_0^\beta d\tau \sum_i (\phi_i^* b_i + b_i^* \phi_i) \right\}. \quad (166)$$

Substituting (166) into (159) gives

$$\mathcal{Z} \propto \int \mathcal{D}[\phi^*, \phi] \exp \left\{ - \int_0^\beta d\tau \phi^\dagger t^{-1} \phi \right\} \int \mathcal{D}[b^*, b] \exp \left\{ -S_{\text{loc}}[b^*, b] + \int_0^\beta d\tau \sum_i (\phi_i^* b_i + b_i^* \phi_i) \right\}. \quad (167)$$

Key simplification — the b -integral factorizes over sites. Since $S_{\text{loc}} = \sum_i S_{0,i}$ is purely on-site (see Eq. (161)), and the source term $\sum_i (\phi_i^* b_i + b_i^* \phi_i)$ is also on-site, the functional integral over b splits into a product of independent single-site integrals:

$$\int \mathcal{D}[b^*, b] e^{-S_{\text{loc}} + \int (\phi^* b + b^* \phi)} = \prod_i \underbrace{\int \mathcal{D}[b_i^*, b_i] \exp \left\{ -S_{0,i}[b_i^*, b_i] + \int_0^\beta d\tau (\phi_i^* b_i + b_i^* \phi_i) \right\}}_{\equiv \mathcal{Z}_{\text{loc}}[\phi_i^*, \phi_i]}. \quad (168)$$

Therefore,

$$\boxed{\mathcal{Z} \propto \int \mathcal{D}[\phi^*, \phi] e^{-S_{\text{eff}}[\phi^*, \phi]}, \quad S_{\text{eff}}[\phi^*, \phi] = \int_0^\beta d\tau \phi^\dagger t^{-1} \phi - \sum_i \ln \mathcal{Z}_{\text{loc}}[\phi_i^*, \phi_i].} \quad (169)$$

Equation (169) is *exact*: no approximation has been made beyond the HS rewriting (which is an identity).

Interpretation of ϕ

The auxiliary field $\phi_i(\tau)$ couples linearly to $b_i(\tau)$, so it acts as a source for local boson coherence. At the saddle point (mean-field level), varying S_{eff} yields a self-consistency relation of the schematic form $\phi \sim t \langle b \rangle$, so ϕ is naturally identified with the superfluid order parameter.

C. Cumulant expansion of $-\ln \mathcal{Z}_{\text{loc}}$: generating Landau terms

To obtain a practical EFT, we expand S_{eff} for small and slowly varying ϕ . This is justified near the transition because the order parameter becomes small, and because we focus on low frequencies and long wavelengths.

We consider first the local partition function \mathcal{Z}_{loc} :

$$\mathcal{Z}_{\text{loc}}[\phi^*, \phi] \equiv \int \mathcal{D}[b^*, b] \exp \left\{ -S_0[b^*, b] + \int_0^\beta d\tau (\phi^*(\tau) b(\tau) + b^*(\tau) \phi(\tau)) \right\}. \quad (170)$$

Here the “site index” i is omitted because each site is identical.

Write the local generating functional as an expectation value in the $\phi = 0$ local theory:

$$\mathcal{Z}_{\text{loc}}[\phi^*, \phi] = \mathcal{Z}_0 \langle e^{X[\phi]} \rangle_0, \quad \text{where } X[\phi] \equiv \int_0^\beta d\tau (\phi^* b + b^* \phi), \quad (171)$$

where $\langle \dots \rangle_0$ denotes averaging with respect to the single-site action S_0 (i.e. the atomic-limit theory).

Local partition function as a source average in the atomic limit

Setting the HS source to zero, $\phi = 0$, the *atomic-limit* (single-site) partition function is

$$\mathcal{Z}_0 \equiv \int \mathcal{D}[b^*, b] e^{-S_0[b^*, b]}.$$

Expectation values $\langle \cdots \rangle_0$ are defined with respect to this $\phi = 0$ local theory:

$$\langle O[b^*, b] \rangle_0 \equiv \frac{1}{\mathcal{Z}_0} \int \mathcal{D}[b^*, b] O[b^*, b] e^{-S_0[b^*, b]}.$$

Therefore, for a generic source term $X[\phi]$,

$$\mathcal{Z}_{\text{loc}}[\phi] = \int \mathcal{D}[b^*, b] e^{-S_0[b^*, b]} e^{X[\phi]} = \mathcal{Z}_0 \underbrace{\frac{1}{\mathcal{Z}_0} \int \mathcal{D}[b^*, b] e^{-S_0[b^*, b]} e^{X[\phi]}}_{\langle e^{X[\phi]} \rangle_0} = \mathcal{Z}_0 \langle e^{X[\phi]} \rangle_0.$$

Using the cumulant (linked-cluster) expansion,

$$\ln \langle e^X \rangle_0 = \sum_{n=1}^{\infty} \frac{1}{n!} \langle X^n \rangle_{0,c}, \quad (172)$$

we obtain

$$-\ln \mathcal{Z}_{\text{loc}}[\phi^*, \phi] = -\ln \mathcal{Z}_0 - \sum_{n=1}^{\infty} \frac{1}{n!} \langle X^n \rangle_{0,c}. \quad (173)$$

Cumulant (linked-cluster) expansion

Let $\langle \cdots \rangle_0$ be any normalized average, $\langle 1 \rangle_0 = 1$, and let X be a (possibly functional) random variable under this measure. Introduce the moment-generating function

$$M(\lambda) \equiv \langle e^{\lambda X} \rangle_0, \quad M(0) = 1. \quad (174)$$

Expanding the exponential and using linearity of $\langle \cdots \rangle_0$, we obtain the *moment* expansion

$$M(\lambda) = \sum_{n=0}^{\infty} \frac{\lambda^n}{n!} \langle X^n \rangle_0. \quad (175)$$

Define the cumulant-generating function as the logarithm

$$W(\lambda) \equiv \ln M(\lambda) = \ln \langle e^{\lambda X} \rangle_0. \quad (176)$$

Since $W(\lambda)$ is analytic around $\lambda = 0$, it admits a Taylor expansion

$$W(\lambda) = \sum_{n=1}^{\infty} \frac{\lambda^n}{n!} \kappa_n, \quad \kappa_n \equiv \left. \frac{d^n W}{d\lambda^n} \right|_{\lambda=0}. \quad (177)$$

The coefficients κ_n are, by definition, the *cumulants* (connected moments), conventionally denoted as $\kappa_n = \langle X^n \rangle_{0,c}$. Setting $\lambda = 1$ gives the cumulant (linked-cluster) expansion

$$\ln \langle e^X \rangle_0 = \sum_{n=1}^{\infty} \frac{1}{n!} \langle X^n \rangle_{0,c}. \quad (178)$$

We now work out the lowest-order cumulants explicitly. Write $W(\lambda) \equiv \ln\langle e^{\lambda X}\rangle_0$ so that $\langle X^n \rangle_{0,c} = \frac{d^n W}{d\lambda^n}|_{\lambda=0}$. Using $\frac{d}{d\lambda}\langle e^{\lambda X}\rangle_0 = \langle X e^{\lambda X}\rangle_0$, one finds

$$\langle X \rangle_{0,c} = W'(0) = \langle X \rangle_0 , \quad (179)$$

$$\langle X^2 \rangle_{0,c} = W''(0) = \langle X^2 \rangle_0 - \langle X \rangle_0^2 , \quad (180)$$

$$\langle X^3 \rangle_{0,c} = W^{(3)}(0) = \langle X^3 \rangle_0 - 3\langle X^2 \rangle_0 \langle X \rangle_0 + 2\langle X \rangle_0^3 . \quad (181)$$

In particular, if $\langle X \rangle_0 = 0$ (as in the Mott phase where $\langle b \rangle_0 = 0$), the second and third cumulants simplify to $\langle X^2 \rangle_{0,c} = \langle X^2 \rangle_0$ and $\langle X^3 \rangle_{0,c} = \langle X^3 \rangle_0$.

In the Mott phase (and near the transition on the MI side), the unperturbed local ground state has $\langle b \rangle_0 = 0$, so the linear term $\langle X \rangle_{0,c}$ vanishes. The leading nontrivial term is quadratic in ϕ , followed by a quartic term that stabilizes the theory.

C.1 Quadratic term: an exact kernel in frequency space

The second cumulant gives

$$\frac{1}{2}\langle X^2 \rangle_{0,c} = \int_0^\beta d\tau_1 \int_0^\beta d\tau_2 \phi^*(\tau_1) G(\tau_1 - \tau_2) \phi(\tau_2) , \quad (182)$$

where

$$G(\tau) \equiv \langle T_\tau b(\tau) b^\dagger(0) \rangle_0 \quad (183)$$

is the *local* (single-site) bosonic Green's function in the atomic limit. Substituting into (169), the quadratic part of the effective action reads¹⁵

$$S_{\text{eff}}^{(2)} = \int_0^\beta d\tau \phi^\dagger t^{-1} \phi - \sum_i \int_0^\beta d\tau_1 \int_0^\beta d\tau_2 \phi_i^*(\tau_1) G(\tau_1 - \tau_2) \phi_i(\tau_2) . \quad (184)$$

This expression is already very informative: the first term couples different lattice sites (via t^{-1}), while the second term is purely on-site but nonlocal in τ .

From $X[\phi]$ to the quadratic kernel $\phi^* G \phi$

Recall the source term on a single site

$$X[\phi] \equiv \int_0^\beta d\tau [\phi^*(\tau) b(\tau) + b^\dagger(\tau) \phi(\tau)] .$$

The quadratic contribution in the cumulant expansion is $\frac{1}{2}\langle X^2 \rangle_{0,c}$. In the Mott (atomic) theory one has $\langle b \rangle_0 = 0$, hence $\langle X \rangle_{0,c} = \langle X \rangle_0 = 0$ and $\langle X^2 \rangle_{0,c} = \langle X^2 \rangle_0$.

Preliminary: Time ordering.

T_τ denotes *imaginary-time ordering*: it rearranges operators such that the one with larger τ appears to the left. For bosons this introduces no extra minus signs.

Derivation.

¹⁵Here the upper index (n) means the n -th power term.

Expanding X^2 and inserting T_τ ,

$$\begin{aligned}\langle X^2 \rangle_0 &= \int_0^\beta d\tau_1 \int_0^\beta d\tau_2 \left\langle T_\tau (\phi_1^* b_1 + b_1^\dagger \phi_1) (\phi_2^* b_2 + b_2^\dagger \phi_2) \right\rangle_0 \\ &= \int d\tau_1 d\tau_2 \left[\phi_1^* \phi_2^* \langle T_\tau b_1 b_2 \rangle_0 + \phi_1 \phi_2 \langle T_\tau b_1^\dagger b_2^\dagger \rangle_0 \right. \\ &\quad \left. + \phi_1^* \phi_2 \langle T_\tau b_1 b_2^\dagger \rangle_0 + \phi_1 \phi_2^* \langle T_\tau b_1^\dagger b_2 \rangle_0 \right],\end{aligned}$$

where $b_a \equiv b(\tau_a)$, $\phi_a \equiv \phi(\tau_a)$. Because the atomic-limit action S_0 preserves the $U(1)$ symmetry $b \rightarrow e^{i\theta} b$, correlators that change particle number vanish:

$$\langle T_\tau b_1 b_2 \rangle_0 = 0, \quad \langle T_\tau b_1^\dagger b_2^\dagger \rangle_0 = 0.$$

Thus only the number-conserving contractions remain. Define the local bosonic Green's function

$$G(\tau) \equiv \langle T_\tau b(\tau) b^\dagger(0) \rangle_0.$$

Using time-translation invariance of S_0 , $\langle T_\tau b(\tau_1) b^\dagger(\tau_2) \rangle_0 = G(\tau_1 - \tau_2)$. Moreover, the last term can be rewritten by exchanging $\tau_1 \leftrightarrow \tau_2$:

$$\int d\tau_1 d\tau_2 \phi_1 \phi_2^* \langle T_\tau b_1^\dagger b_2 \rangle_0 = \int d\tau_1 d\tau_2 \phi_1^* \phi_2 \langle T_\tau b_1 b_2^\dagger \rangle_0.$$

Combining the two equal contributions, we obtain the compact kernel form

$$\frac{1}{2} \langle X^2 \rangle_{0,c} = \int_0^\beta d\tau_1 \int_0^\beta d\tau_2 \phi^*(\tau_1) G(\tau_1 - \tau_2) \phi(\tau_2).$$

It is convenient to Fourier transform in time and space. Define Matsubara components $\phi_i(\tau) = \frac{1}{\sqrt{\beta N}} \sum_{k, \omega_n} e^{i(k \cdot r_i - \omega_n \tau)} \phi(k, \omega_n)$, with bosonic Matsubara frequencies $\omega_n = 2\pi n/\beta$. Then (184) becomes

$$S_{\text{eff}}^{(2)} = \sum_{k, \omega_n} \phi^*(k, \omega_n) \left[t(k)^{-1} - G(i\omega_n) \right] \phi(k, \omega_n), \quad (185)$$

where $t(k)$ is the lattice Fourier transform of t_{ij} , and $G(i\omega_n) = \int_0^\beta d\tau e^{i\omega_n \tau} G(\tau)$.

C.2 Explicit evaluation of $G(i\omega_n)$ in the atomic limit

For the Bose–Hubbard local Hamiltonian $\hat{H}_0 = \frac{U}{2} \hat{n}(\hat{n} - 1) - \mu \hat{n}$, the eigenstates are number states $|n\rangle$ with energies

$$E_n = \frac{U}{2} n(n-1) - \mu n. \quad (186)$$

In the n_0 -th Mott lobe, the local ground state is $|n_0\rangle$. The dominant intermediate states created by b^\dagger and b are $|n_0 + 1\rangle$ and $|n_0 - 1\rangle$, with excitation energies

$$E_p \equiv E_{n_0+1} - E_{n_0} = Un_0 - \mu, \quad E_h \equiv E_{n_0-1} - E_{n_0} = \mu - U(n_0 - 1). \quad (187)$$

Using $\langle n_0 + 1 | b^\dagger | n_0 \rangle = \sqrt{n_0 + 1}$ and $\langle n_0 - 1 | b | n_0 \rangle = \sqrt{n_0}$, a standard spectral decomposition yields

$$G(i\omega_n) = \frac{n_0 + 1}{E_p - i\omega_n} + \frac{n_0}{E_h + i\omega_n}. \quad (188)$$

In particular,

$$G(0) = \frac{n_0 + 1}{E_p} + \frac{n_0}{E_h}. \quad (189)$$

Derivation of the atomic-limit Green's function $G(i\omega_n)$

In the atomic limit ($\phi = 0$), the local Hamiltonian $\hat{H}_0 = \frac{U}{2}\hat{n}(\hat{n}-1) - \mu\hat{n}$ is diagonal in number states $|n\rangle$ with energies E_n . In the n_0 -th Mott lobe (low temperature, $\beta E_{p/h} \gg 1$), we may approximate thermal averages by the local ground state $|n_0\rangle$:

$$\langle \cdots \rangle_0 \simeq \langle n_0 | \cdots | n_0 \rangle.$$

Define the (bosonic) Matsubara Green's function

$$G(\tau) \equiv \langle T_\tau b(\tau) b^\dagger(0) \rangle_0, \quad b(\tau) = e^{\tau\hat{H}_0} b e^{-\tau\hat{H}_0}.$$

Step 1: spectral decomposition in imaginary time. For $0 < \tau < \beta$, time ordering is trivial and

$$\begin{aligned} G(\tau) &= \langle n_0 | b(\tau) b^\dagger(0) | n_0 \rangle = \sum_m \langle n_0 | e^{\tau\hat{H}_0} b e^{-\tau\hat{H}_0} | m \rangle \langle m | b^\dagger | n_0 \rangle \\ &= \sum_m e^{-\tau(E_m - E_{n_0})} \langle n_0 | b | m \rangle \langle m | b^\dagger | n_0 \rangle. \end{aligned}$$

Since $b^\dagger |n_0\rangle = \sqrt{n_0 + 1} |n_0 + 1\rangle$, only $m = n_0 + 1$ contributes, giving

$$G(\tau) = (n_0 + 1) e^{-E_p \tau}, \quad E_p \equiv E_{n_0+1} - E_{n_0}.$$

For $-\beta < \tau < 0$, time ordering swaps the operators, $G(\tau) = \langle n_0 | b^\dagger(0) b(\tau) | n_0 \rangle$, and similarly only $m = n_0 - 1$ contributes because $b |n_0\rangle = \sqrt{n_0} |n_0 - 1\rangle$, yielding

$$G(\tau) = n_0 e^{E_h \tau}, \quad E_h \equiv E_{n_0-1} - E_{n_0}.$$

Using bosonic periodicity $G(\tau + \beta) = G(\tau)$, for $0 < \tau < \beta$ one may equivalently write

$$G(\tau) = (n_0 + 1) e^{-E_p \tau} + n_0 e^{-E_h (\beta - \tau)}.$$

Step 2: Matsubara transform. With $\omega_n = 2\pi n/\beta$,

$$\begin{aligned} G(i\omega_n) &\equiv \int_0^\beta d\tau e^{i\omega_n \tau} G(\tau) \\ &= (n_0 + 1) \int_0^\beta d\tau e^{-(E_p - i\omega_n)\tau} + n_0 \int_0^\beta d\tau e^{i\omega_n \tau} e^{-E_h (\beta - \tau)} \\ &= (n_0 + 1) \frac{1 - e^{-\beta(E_p - i\omega_n)}}{E_p - i\omega_n} + n_0 \frac{e^{i\omega_n \beta} - e^{-\beta E_h}}{E_h + i\omega_n}. \end{aligned}$$

For bosonic ω_n , $e^{i\omega_n \beta} = 1$. In the Mott regime $\beta E_{p/h} \gg 1$, the Boltzmann factors $e^{-\beta E_{p/h}}$ are negligible, and we obtain

$$G(i\omega_n) = \frac{n_0 + 1}{E_p - i\omega_n} + \frac{n_0}{E_h + i\omega_n}.$$

C.3 Quartic term: local $|\phi|^4$ from the connected 4-point function

The next nonvanishing contribution is the connected fourth cumulant $\langle X^4 \rangle_{0,c}$, which produces a local quartic term. Keeping only the low-frequency component (static, slowly varying ϕ), one obtains the standard Landau stabilization

$$S_{\text{eff}}^{(4)} \approx \int_0^\beta d\tau \sum_i b |\phi_i(\tau)|^4, \quad b > 0, \quad (190)$$

where the constant b is determined by the on-site connected four-point correlator in the atomic limit. (For the purpose of deriving long-wavelength scaling, its explicit form is usually not needed.)

D. Long-wavelength expansion: deriving the derivative EFT

Equation (185) shows that the quadratic theory is governed by the kernel

$$\mathcal{K}(\mathbf{k}, i\omega_n) \equiv t(\mathbf{k})^{-1} - G(i\omega_n). \quad (191)$$

The long-wavelength/low-frequency EFT is obtained by Taylor expanding \mathcal{K} around $(\mathbf{k}, \omega) = (0, 0)$, and then Fourier transforming back to real space.

D.1 Spatial gradient term from $t(\mathbf{k})^{-1}$

For nearest-neighbor hopping on a regular lattice, $t(\mathbf{k}) = J\gamma_k$, where γ_k is the lattice structure factor with $\gamma_0 = Z$. Expanding for small $|\mathbf{k}|$,

$$t(\mathbf{k}) = J\gamma_k \simeq J \left(Z - c a_0^2 k^2 + \dots \right), \quad (k \equiv |\mathbf{k}|), \quad (192)$$

where a_0 is the lattice spacing and $c = O(1)$ depends on lattice geometry. Therefore,

$$t(\mathbf{k})^{-1} \simeq \frac{1}{ZJ} + \frac{c a_0^2}{Z^2 J} k^2 + \dots. \quad (193)$$

Upon Fourier transforming back to real space, the k^2 term gives a gradient contribution¹⁶

$$\int d\tau d^d r w |\nabla \phi|^2, \quad w \sim \frac{c a_0^2}{Z^2 J}, \quad (194)$$

up to a convention-dependent rescaling of ϕ .

D.2 Temporal derivative terms from the ω -expansion of $G(i\omega)$

Using (188), expand $G(i\omega)$ for small ω :

$$\begin{aligned} \frac{1}{E_p - i\omega} &= \frac{1}{E_p} + \frac{i\omega}{E_p^2} + \frac{(i\omega)^2}{E_p^3} + O(\omega^3), \\ \frac{1}{E_h + i\omega} &= \frac{1}{E_h} - \frac{i\omega}{E_h^2} + \frac{(i\omega)^2}{E_h^3} + O(\omega^3). \end{aligned} \quad (195)$$

Hence

$$G(i\omega) = G(0) + \left(\frac{n_0 + 1}{E_p^2} - \frac{n_0}{E_h^2} \right) i\omega + \left(\frac{n_0 + 1}{E_p^3} + \frac{n_0}{E_h^3} \right) (i\omega)^2 + O(\omega^3). \quad (196)$$

¹⁶Here we use w as the coefficient of $|\nabla \phi|^2$. Don't mix up with the frequency ω .

Substituting into (191) and Fourier transforming back to time, the ω -linear term generates a first-order temporal derivative $u\phi^*\partial_\tau\phi$, while the ω^2 term generates $v|\partial_\tau\phi|^2$. Up to overall sign conventions (depending on how one writes the Berry-phase term in the microscopic action), the coefficients are proportional to

$$u \propto -\left(\frac{n_0 + 1}{E_p^2} - \frac{n_0}{E_h^2}\right), \quad v \propto -\left(\frac{n_0 + 1}{E_p^3} + \frac{n_0}{E_h^3}\right). \quad (197)$$

D.3 Mass term and the transition criterion

The constant part of the kernel gives the Landau mass term. At $k = 0$, $t(\mathbf{0}) = ZJ$, so

$$\mathcal{K}(\mathbf{0}, 0) = \frac{1}{ZJ} - G(0). \quad (198)$$

With the Landau convention that the action contains $-a|\phi|^2$, we identify

$$a = G(0) - \frac{1}{ZJ} = \frac{n_0 + 1}{Un_0 - \mu} + \frac{n_0}{\mu - U(n_0 - 1)} - \frac{1}{ZJ}. \quad (199)$$

The phase boundary is determined by $a = 0$, which reproduces the mean-field instability condition for the Mott phase.

D.4 Final derivative-expanded EFT

Combining the above ingredients and retaining the leading local quartic term, we arrive at the continuum long-wavelength EFT

$$S_{\text{EFT}}[\phi^*, \phi] = \int_0^\beta d\tau \int d^d r [u\phi^*\partial_\tau\phi + v|\partial_\tau\phi|^2 + w|\nabla\phi|^2 - a|\phi|^2 + b|\phi|^4 + \dots], \quad (200)$$

where the coefficients a, u, v, w, b are determined (in principle exactly, and in practice approximately) by local correlation functions of the atomic-limit theory together with the small- k expansion of the hopping matrix $t(k)$.

What is “long-wavelength” here? (conditions of validity)

The derivative expansion assumes that $\phi(r, \tau)$ varies slowly compared to microscopic scales:

$$|\omega| \ll E_p, E_h, \quad |\mathbf{k}| \ll a_0^{-1},$$

so that the kernel $\mathcal{K}(k, i\omega)$ is analytic near $(0, 0)$ and can be Taylor expanded. Close to the particle-hole symmetric line (near the lobe tip) the coefficient u may become small, and the $v|\partial_\tau\phi|^2$ term becomes essential; away from that regime the u -term typically dominates the temporal dynamics.